Copper(I) 1,1-dithiolate cluster transformations. Synthesis of $[Bu_4N]_6[Cu_6(S,i\text{-}MNT)_6]$, $i\text{-}MNT = [S_2CC(CN)_2]^-$, from $[Bu_4N]_4[Cu_8(i\text{-}MNT)_6]$ with sulfur. Reaction of the cyclic hexanuclear complex with phosphine to give the tetrahedral $[Bu_4N]_4[Cu_4(i\text{-}MNT)_4]$ which oxidizes in solution to give the homocubane $[Bu_4N]_4[Cu_8(i\text{-}MNT)_6]$ and $[Bu_4N]_2[Cu(i\text{-}MNT)_2]$

C.W. Liu, Richard J. Staples, John P. Fackler [1] *

*Laboratory for Molecular Structure and Bonding, Department of Chemistry,
Texas A & M University, College Station, TX 77842-3012, USA*

Contents

* Corresponding author. Fax: (409) 845-9351; e-mail: Fackler@chemvx.tamu.edu

Abstract

The novel sulfur-rich cluster anion, $[Cu_6(S,i\text{-MNT})_6]^{6-}$, **2**, is obtained from the reaction of the homocubane, $[Cu_8(i\text{-MNT})_6]^{4-}$, **1**, and powdered sulfur in acetonitrile solution under basic conditions. Compound **2** crystallizes in the $R\bar{3}$ space group with $a = 33.519(5)$ Å, $b = 33.519(5)$ Å, $c = 11.748(2)$ Å, $\gamma = 120°$, and $V = 11431(3)$ Å^3. The molecule contains six trigonally coordinated copper atoms linked together into a 12 membered ring by the six sulfur atoms of the bridging sulfur-rich i-MNT ligands. Six Cu^I atoms are located at the vertices of a nearly regular hexagon. The mean distance between the two planes of alternating Cu^I atoms is 0.345(2) Å. When **2** reacts with triphenylphosphine, a sulfur atom is removed from the disulfide containing ligands to give $[Cu_4(i\text{-MNT})_4]^{4-}$, isolated as the $[^nBu_4N]^+$ salt, **4**. This tetranuclear species also can be synthesized directly from $[Cu(CH_3CN)_4][PF_6]$ and $[^nBu_4N]_2[i\text{-MNT}]$ in acetonitrile. Compound **4** crystallizes in the $C2/c$ space group with $a = 38.351(6)$ Å, $b = 38.468(8)$ Å, $c = 32.685(5)$ Å, $\beta = 124.94(1)°$, and $V = 39527(12)$ Å^3. The anion reveals discrete units of four copper atoms at the vertices of a distorted tetrahedron, bound to four i-MNT groups acting as "tridentate" (μ_1, μ_2) ligands. The cluster anion also is found as $[BzEt_3N][^nBu_4N]_3[Cu_4(i\text{-MNT})_4]$, **5**. Compound **5** crystallizes in the $C2/c$ space group with $a = 27.306(7)$ Å, $b = 14.127(3)$ Å, $c = 27.868(6)$ Å, $\beta = 121.22(2)°$, and In solution the tetranuclear species transforms with oxidation into the Cu$_8$ homocubane, **1**, and the paramagnetic anion $[Cu^{II}(i\text{-MNT})_2]^{2-}$, isolated as the $[^nBu_4N]^+$ salt, **3**. Spectroscopic evidence, including UV–Vis and ^{13}C–NMR, for the cluster transformation is presented. Compound **3** crystallizes in the $P2_1/n$ space group with $a = 10.036(1)$, $b = 16.724(2)$, $c = 14.234(1)$, $\beta = 91.37(9)$, and $V = 2388(0)$. The anion in **3** is planar with the copper atom located on the center of symmetry. Pertinent ^{13}C chemical shifts (ppm) and absorption maxima (nm) with extinction coefficients in parentheses are as follows: **1**, 14, 20, 24, 59, 79.8, 116.5, 197.7; 404 ($\epsilon = 86\,000$ M^{-1} cm^{-1}), 320 ($\epsilon = 60\,000$ M^{-1} cm^{-1}). **2**, 14, 20, 24, 59, 61.7, 118.5, 119.5, 158; 380 ($\epsilon = 85\,000$ M^{-1} cm^{-1}), 350 sh ($\epsilon = 74\,000$ M^{-1} cm^{-1}). **3**, 450 ($\epsilon = 15\,000$ M^{-1} cm^{-1}), 350 ($\epsilon = 80\,000$ M^{-1} cm^{-1}), 340 sh ($\epsilon = 43\,000$ M^{-1} cm^{-1}), 315 sh ($\epsilon = 25\,000$ M^{-1} cm^{-1}). **4**, 14, 20, 24, 59, 70.8, 120, 209.5; 380 ($\epsilon = 92\,000$ M^{-1} cm^{-1}). © 1998 Elsevier Science S.A. All rights reserved.

1. Introduction

The critical role of copper in biological system has been recognized for a long time. Copper is an essential component for living systems, although excess intake

can be toxic as in Wilson's disease [1]. A copper-deficiency disease, Menkes disease [2], a rare neurological disorder that generally kills children by age three, is also known.

The chemistry of clusters of copper(I) with sulfur ligands is extremely important in life systems [3]. Many technologies also utilize Cu^I–S clusters [4,5]. Yet the structure types, the bonding, and the cluster redox properties of Cu^I–S clusters are rather incompletely understood. Recently it has been determined that yeast and mammalian metallothioneins (MT), proteins which contain a Cu^I–S cluster, function as anti-oxidants [6]. With copper and mammalian MT it appears that $Cu_6(S$–$Cys)_{11}$ and $Cu_6(S$–$Cys)_9$ clusters form [7–11]; a trigonal prismatic model for $Cu_6(S$–$Cys)_9$ has been proposed [7,8]. Structural studies suggest that yeast MT may contain a cluster of eight Cu^I ions coordinated with 12 sulfur atoms from cysteine residues [12,13]. Its expression is regulated by a protein CUP2 (also known as ACE1) which also appears to be a Cu^I–S cluster, although its detailed structure is unknown [14].
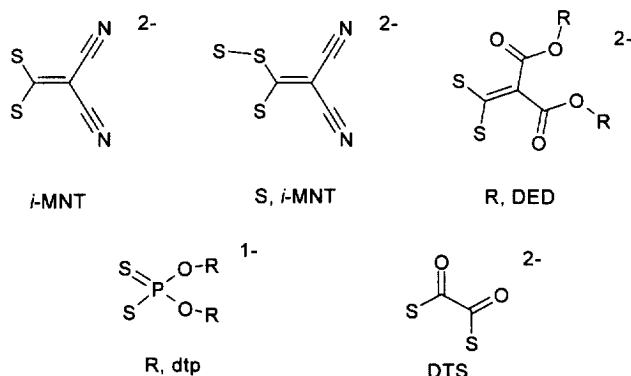
The $Cu_8^I S_{12}$ homocubane cluster geometry reported by McCandlish et al. [15] over 25 years ago contains structural features similar to those observed in various Cu^I–S proteins. This fact makes the Cu_8S_{12} homocubane much more relevant as a structural type in biology than when it first discovered. Furthermore, centered cubanes of Cu^I such as [$Cu_8(dtp)_6S$], dtp = dialkyldithiophosphate, have been synthesized (see the scheme of the ligands above) and structurally characterized recently [16,17]. These compounds appear to be related structurally to the "basic" dithioacetates and dithiophosphates such as [$Zn_4(dtp)_6S$] [18]. The cluster anion of 1, [$Cu_8(i$-$MNT)_6]^{4-}$, consists of a slightly distorted cube of copper atoms embedded within the 12 sulfur atoms which lie on the vertices of a distorted icosahedron. The overall symmetry of the anion approximates the point group T_h. In 1, all of the S atoms bridge to two Cu^I atoms while the coordination about each Cu^I atom is approximately trigonally planar.

Upon "oxidation" of a homocubane dithiolate cluster with sulfur, Coucouvanis et al. [19,20] established that a sulfur atom is added to each ligand. While no solid-state structural data were obtained for a "sulfur-rich" homocubane, solution

$^{13}C\{^1H\}$ NMR results when non-interacting $[^nBu_4N]^+$ cations were used suggested that several isomers formed in which sulfur atoms were added to the dithiolate ligands [19]. With alkali metal cations, a "sulfur-rich" tetranuclear product with a stoichiometry of one-half that of the "sulfur-rich" homocubane, is formed. This material, $[Cu_4(S,L)_3]^{2-}$, structurally characterized in the $(Ph_4P)K[Cu_4(S, {}^tBu-DED)_3]$ cluster, contains the Cu_4S_6 cluster core in which each edge of a Cu_4 tetrahedron contains a bridging S atom [20]. Structural evidence also was obtained by Coucouvanis et al. [21,22] for the formation of tetrahedral clusters when proton acids were reacted with the homocubane clusters. The cluster $[Cu_{10}(H-{}^tBu-DED)_6({}^tBu-DED)_2]$ has two tetrahedral Cu_4S_8 clusters linked by two trigonal CuS_2O units. Spectroscopic evidence was presented for protonation of one of the olefinic carbon atoms of the dithiolate ligands as the cause for the cluster rearrangement [21,22].

Two observations have prompted us to re-examine the Cu^I–S dithiolate cluster chemistry. First, there is a strong interest in the redox properties of Cu^I–S clusters in both biology and the chemical industry [3,4]. The generality of the sulfur addition process with homocubane dithiolates of Cu^I and Ag^I remains uncertain. The sulfur addition reaction to $[Cu_8(i\text{-}MNT)_6]^{4-}$ surprisingly produced a new "sulfur-rich" cluster $[^nBu_4N]_6[Cu_6(S,i\text{-}MNT)_6]$, **2**, which has been structurally characterized, a species which has a nearly planar hexagonal arrangement of Cu^I atoms. Second, in view of the importance of cubane Cu_8S_{12} clusters as possible synthetic models of the protein CUP1 sites, an investigation directed toward developing an understanding of the reaction sequences which lead to the cubane formation was undertaken. The synthesis and structural characterization of paramagnetic $[^nBu_4N]_2[Cu^{II}(i\text{-}MNT)_2]$, **3**, and the preparation of $[^nBu_4N]_4[Cu_4(i\text{-}MNT)_4]$, **4**, containing a tetrahedral copper core with a structure similar to that [23] of $Cu_4(dtc)_4$, dtc = diethyldithiocarbamate, have contributed to this study. Both species are detectable, isolable components in the formation of the octanuclear $[Cu_8(i\text{-}MNT)_6]^{4-}$ cluster.

Detailed synthetic and X-ray structural results of compounds **2**, **3**, and **4** are presented here along with the spectroscopic evidence for the direct formation of the homocubane from the tetranuclear species. A preliminary report of the structure of **2** has been reported [24].

2. Experimental section

All reactions were carried out in oven-dried Schlenk glassware by using standard inert-atmosphere techniques [25]. Commercial acetonitrile and acetone were distilled from P_4O_{10} and $K_2CO_3/KMnO_4$, respectively, before use. Methanol was distilled from Mg. Ether was distilled from Na/K. All infrared spectra were recorded on a Perkin–Elmer 783 spectrometer at 20 °C using either CsI (200–4000 cm^{-1}) or KBr plates. UV–visible studies were carried out on a Cary 17 spectrophotometer. NMR spectra were recorded on a Varian XL-200 Fourier transform spectrometer. The $^{31}P\{^1H\}$ NMR were referenced externally against H_3PO_4. $^{13}C\{^1H\}$ NMR were referenced against the deuterated form of the solvent. EPR spectra were recorded on a Bruker ESP 300 equipped with an Oxford ER910A cryostat operating at 100 K.

Samples were typically 10^{-5} M in 1,2-dichloroethane, frozen in liquid N_2 and then cooled to 100 K. The ^{252}Cf-plasma desorption mass spectra (PDMS) were obtained on an instrument developed at Texas A & M University (equipment developed by R. D. Mccfarlane). Elemental analyses were performed by Galbraith Laboratories, Knoxville, TN. Melting points were measured on a Thomas Hoover capillary melting point apparatus. [Cu(CH$_3$CN)$_4$]PF$_6$, [26] and [Bu$_4$N]$_2$[Cu(i-MNT)$_2$], 3 [27,28], were prepared according to literature procedures. $C_2H_4Cl_2$ (spectroscopic grade), PPh$_3$ and sulfur powder were commercially available (Aldrich) and used without further purification. KOH(aq) was standardized using potassium hydrogen phthalate.

2.1. Syntheses

2.1.1. Tetrakis(tetra-n-butylammonium)hexakis (1,1-dicyanoethylene-2,2-dithiolato) octacopper(i), [Bu$_4$N]$_4$[Cu$_8$(i-MNT)$_6$]

The preparation of compound 1 followed the procedure for the synthesis of (PhMe$_3$N)$_4$[Cu$_8$(i-MNT)$_6$] [15]. The orange-red crystalline material was obtained by recrystallizing in acetone (90% yield); mp 270 °C dec, IR, cm^{-1}: v(CN), 2205(s). ^{13}C NMR(CD$_3$CN): 14, 20, 24, 59, 79.8, 116.5, 197.7 ppm. PDMS, m/e: 2563 ($M_{calc}^+ = 2562$), Anal. Calcd for $C_{88}H_{144}N_{16}S_{12}Cu_8$: C, 45.61; H, 6.21; N, 9.67; S,16.58. Found: C, 45.24; H, 6.31; N, 9.46; S, 16.23.

2.1.2. Hexakis(tetra-n-butylammonium)hexakis (1,1-dicyanoethylene-2-thio,2'-perthiolato) hexacopper(i), [Bu$_4$N]$_6$[Cu$_6$(S,i-MNT)$_6$]

[Bu$_4$N]$_4$[Cu$_8$(i-MNT)$_6$] (0.09 mmol) was dissolved in 10 mL of acetonitrile and sulfur powder (1.08 mmol) was added with stirring. The solution changed color instantly from red to dark-red after adding KOH(aq) (5 ml, 0.66 N). After being stirred for 12 h, the solution was filtered, and most of the solvent was removed by rota-evaporation under reduced pressure. The crude product was precipitated by adding 15 ml H_2O. The solid was isolated, washed with Et$_2$O, and redissolved in CH$_2$Cl$_2$. The orange-yellow crystalline material was obtained by recrystallizing in CH$_2$Cl$_2$ (40% yield); mp 165 °C dec., IR, cm^{-1}: v(CN), 2185(s), 2160(s); v(S–S), 460(s). ^{13}C NMR(Acetone-d_6): 14, 20, 24, 59, 61.7, 118.5, 119.5, 158 ppm. Anal. Calcd for $C_{120}H_{216}N_{18}S_{18}Cu_6$; C, 50.28; H, 7.54; N, 8.79; S, 20.13. Found: C, 50.94; H, 7.12; N, 8.23; S, 19.58.

2.1.3. [tetrakis(tetra-n-butylammonium)][tetrakis(1,1-dicyanoethylene-2,2-dithiolato)tetracopper(i)], [Bu$_4$N]$_4$[Cu$_4$(i-MNT)$_4$]

Method A. [Bu$_4$N]$_6$[Cu$_6$(S,i-MNT)$_6$], 2, (0.08 mmol) was dissolved in 20 ml of acetone and PPh$_3$ (0.48 mmol) was added with stirring. After stirring for 1 h, the solution was filtered, and the solvent was removed by rota-evaporation under reduced pressure. The crude product was washed with copious amounts of ether to remove SPPh$_3$. The yellow powder was obtained in 70% yield; mp 240 °C dec.

Method B. [Cu(CH$_3$CN)$_4$]PF$_6$ (0.1 mmol) and [Bu$_4$N]$_2$[i-MNT] (0.1 mmol) were dissolved in 30 ml of acetonitrile and stirred for 24 h. The solution was filtered and

most of the solvent was removed under vacuum. The yellow residue was washed with ether and redissolved in 30 ml of acetonitrile. Yellow crystals were obtained by recrystallization in acetonitrile solution layered with ether, after a few days (20% yield). Anal. Calcd for $C_{80}H_{144}N_{12}S_8Cu_4$: C, 53.89; H, 8.08; N, 9.42; S, 14.36. Found: C, 53.63; H, 7.91; N, 9.58; S, 14.16. PDMS, m/e: 2030 ($M_{calc}^+ = 2029.64$), ^{13}C NMR, 14, 20, 24, 59, 70.8, 120, 209.5. IR, cm^{-1}: ν(CN), 2180(b).

2.1.4. [benzyltriethylammonium tris(tetra-n-butylammonium)] [tetrakis(1,1-dicyano-ethylene-2,2-dithiolato) tetracopper(i)], [BzEt₃N][Bu₄N]₃[Cu₄(i-MNT)₄]

Compound **5** was prepared by reacting four equivalents of benzyltriethylammonium chloride with compound **4** in methanol solution for 12 h. The solution was filtered, and the solvent was removed under vacuum. The crude product was washed with H_2O to remove the excess quaternary ammonium salts (Yield 40%). Anal. Calcd for $C_{77}H_{130}N_{12}S_8Cu_4$: C, 53.37; H, 7.50; N, 9.70; S, 14.77. Found: C, 53.76; H, 7.70; N, 9.30; S, 14.37.

2.1.5. Monitoring of the conversion reactions

The formation of the $[Cu_8(i\text{-}MNT)_6]^{4-}$ cluster from $[Cu_4(i\text{-}MNT)_4]^{4-}$ was monitored spectroscopically by UV–Vis and by ^{13}C NMR spectroscopy. In a typical experiment, a 10^{-5} M solution of **4** in 1,2-dichloroethane was placed in a 1 cm square quartz cell and placed in a Cary Model 17 spectrophotometer equipped with a thermostated cell holder maintained at 52.0 °C. Spectra were recorded at 1 h intervals throughout the course of the experiment. In a typical ^{13}C NMR measurement, a concentrated solution ($>10^{-1}$ M) of **4** in CD_2Cl_2 was placed in a 10 mm NMR tube in the spectrometer at ambient temperature. It took more than 3 h (7000 transients) to record each spectrum.

2.1.6. X-ray diffraction analysis

Light orange yellow crystals of $[Bu_4N]_6[Cu_6(S,i\text{-}MNT)_6]$, **2**, and red-brown crystals of $[Bu_4N]_2[Cu(i\text{-}MNT)_2]$, **3**, suitable for X-ray diffraction analysis were grown at ambient temperature from a CH_2Cl_2 solution layered with hexane. Yellow crystals of $[Bu_4N]_4[Cu_4(i\text{-}MNT)_4]$, **4**, and $[BzEt_3N][Bu_4N]_3[Cu_4(i\text{-}MNT)_4]$, **5**, were obtained by crystallization in acetone solution layered with hexane at ambient temperature. Crystals were mounted on the end of a glass fiber with epoxy resin. Unit cells were determined from 20 machine-centered reflections obtained from rotation photographs. Refined cell parameters were determined from the setting angles of 25 reflections with $20° < 2\theta < 30°$. Data collection was carried out at ambient temperature using a Nicolet R3/m diffractometer controlled by a Data General Nova 4 minicomputer utilizing the Wycoff scanning technique in a bisecting geometry and graphite-monochromated Mo Kα radiation over the range of $4° < 2\theta < 45°$. Backgrounds were estimated from a 64-step profile. The scan rate was variable, 3–30° min^{-1}, scan width 1.0°, scan offset 1.0°. Three standards measured every 97 data showed no significant variation over the period of data collection.

Data were corrected for absorption, Lorentz and polarization effects. An empirical absorption correction was made on the basis of azimuthal scans of five strong

reflections spanning a range of 2θ values. All data processing was performed by a Data General Eclipse S140 minicomputer using the SHELXTL crystallographic computational package (version 5.1).

The Laue symmetry and systematic absences were consistent with the space group R bar 3 for compound **2**. The initial atomic coordinates for the copper atom in the asymmetric unit of **2** were determined by direct methods, and subsequent atom positions were located on difference Fourier maps. The structure was refined using the SHELXL 93 crystallographic software package [29]. All but the hydrogen atoms were refined anisotropically. The hydrogen atoms on the *n*-butyl group were calculated by using fixed C–H bond lengths, 0.96 Å.

The crystal structure of **3** was solved using direct methods to determine the copper atom position. Subsequently other atom positions were located on difference Fourier maps. The structure was refined using the SHELXL 86 crystallographic software package [30]. All but the hydrogen atoms were refined anisotropically. The hydrogen atoms on the *n*-butyl group were calculated by using fixed C–H bond lengths, 0.96 Å.

Systematic absences narrowed the space group choices to $C2/c$ and Cc for **4** and **5**. The structures were solved in $C2/c$ by direct methods to determine the copper atom positions, while other atom positions were located on difference Fourier maps. Structures **4** and **5** were refined initially using SHELXL-86 with data based on F. Data using SHELXL-93 based on F^2 are reported here. All atoms of the anion were refined anisotropically. The quaternary ammonium cations of **4** and **5** were seriously disordered. Hydrogen atoms were not included. In structure **4**, five carbon atoms of the ammonium salts were not found. The somewhat high, final R values based on F^2 reflect crystals which yielded a relatively weak data set and the presence of disordered ammonium cations.

The crystallographic details are listed in Table 1. Selected bond distances and angles for structures **2–5** are given in Tables 2–5.

3. Results

3.1. Syntheses

The sulfur-rich cluster, $[Bu_4N]_6[Cu_6(S,i\text{-}MNT)_6]$, **2**, is obtained by reacting powdered sulfur and $[Bu_4N]_4[Cu_8(i\text{-}MNT)_6]$, **1**, in acetonitrile solution under basic conditions. The solution color turns deep red which is a general indication of the formation of the polysulfide anion, S_x^{2-}. It is necessary to wash the crude products with H_2O. The $[Bu_4N]_6[Cu_6(S,i\text{-}MNT)_6]$ precipitates when H_2O is added to the basic acetonitrile solution after removal of most of the solvent. The excess polysulfide can be removed by redissolving the crude products in CH_2Cl_2. Single crystals suitable for X-ray crystallography were grown in CH_2Cl_2 layered with hexane. The infrared spectrum of **2** shows many similarities to the spectrum of **1**. The major differences are that **2** shows two CN^- stretching peaks, 2185 and 2160 cm^{-1}, and a peak at 460 cm^{-1} which is reasonably assigned to the sulfur–sulfur stretching vibration.[31] The two CN^- stretching peaks apparently result from the unsymmetrical coordination environment of the *i*-MNT ligands (vide infra). The ^{13}C-NMR spectra also
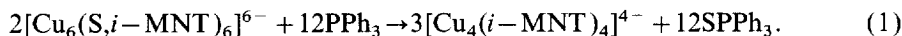
Table 1
Crystallographic data

	2	3	4	5
Formula	$C_{120}H_{216}Cu_6N_{18}S_{18}$	$C_{40}H_{72}CuN_6S_4$	$C_{160}H_{288}Cu_8N_{24}S_{16}$	$C_{77}H_{130}Cu_4N_{12}S_8$
fw	2869.43	828.835	3569.42	1734.57
Space group	$R\bar{3}$	$P2_1/n$	$C2/c$	$C2/c$
a (Å)	33.519(5)	10.036(1)	38.351(6)	27.306(7)
b (Å)	33.519(5)	16.724(2)	38.468(8)	14.127(3)
c (Å)	11.748(2)	14.234(1)	32.685(5)	27.868(6)
α (degrees)	90	90	90	90
β (degrees)	90	91.366(9)	124.94(1)	121.22(2)
γ (degrees)	120	90	90	90
V (Å^3)	11431(3)	2388(1)	39527(12)	9193(4)
Z	3	2	8	4
D_{calc} (Mg/m^3)	1.250	1.152	1.200	1.253
μ(Mo,Kα) (cm^{-1})	11.16	6.56	10.61	11.39
Temp (K)	293(2)	293(2)	293(2)	293(2)
$F(000)$	4572	894	15232	3680
λ(radiation) (Å)	0.71073	0.71073	0.71073	0.71073
transm. factor max, min	0.959, 0.825	0.962, 0.855	0.979, 0.757	0.966, 0.856
Crystal size	$0.5 \times 0.1 \times 0.1$	$0.6 \times 0.3 \times 0.2$	$0.6 \times 0.5 \times 0.2$	$0.2 \times 0.2 \times 0.1$
Goodness-of-fit[a]	1.006 (on F^2)	1.348 (on F)	0.957 (on F^2)	1.021 (on F^2)
$R^b, Rw^b, wR2^b$	0.0599, 0.0845	0.0434, 0.0457	0.1177, 0.3044	0.0840, 0.2150

[a] Goodness-of-fit $= [\Sigma(w|F_0| - |F_c|^2)/(M - N)]^{1/2}$, where M is the number of reflections and N is the number of parameters refined.
[b] $R1 = \Sigma|F_0| - |F_c|/\Sigma|F_0|$; $wR2 = \{\Sigma[w(F_0^2 - F_c^2)^2]/\Sigma[wF_0^4]\}^{1/2}$; $Rw = \{\Sigma[w(F_0 - F_c)^2]/\Sigma[wF_0^2]\}^{1/2}$.

show two resonances, 118.5 and 119.5 ppm, which are assigned to the two cyano carbon atoms of the ligand. The carbon atoms of the CS_2 moiety and olefinic units in **2** show resonances at 158 and 61.7 ppm, respectively, shifted upfield by comparison to the corresponding resonances in the "parent cubane" **1** (197.2 and 79.8 ppm). The electronic spectrum of compound **2** shows an absorption band at 380 nm ($\epsilon = 85\,000$ M^{-1} cm^{-1}) and a shoulder at 350 nm ($\epsilon = 74\,000$ M^{-1} cm^{-1}) in 1,2-dichloroethane. Thus the band observed at 404 nm in compound **1** shows a hypsochromic shift (blue shift) in the sulfur-rich hexanuclear species.

Removal of a sulfur atom from a sulfur-rich ligand by using PPh$_3$ occurs readily [32]. After adding six equivalents of PPh$_3$ into an acetone solution of $[Cu_6(S,i\text{-MNT})_6]^{6-}$, complex **4** could be obtained with high yield (>70% yield based on ^{13}C NMR). One of the reaction products, SPPh$_3$, was isolated from ether filtrates used to wash the residue and identified by ^{31}P{^{1}H} NMR. The desulfurization process is represented by Eq. (1):

$$2[Cu_6(S,i-MNT)_6]^{6-} + 12PPh_3 \rightarrow 3[Cu_4(i-MNT)_4]^{4-} + 12SPPh_3. \qquad (1)$$

The infrared spectrum of **4** shows one CN$^-$ stretching peak at 2180 cm^{-1}. The electronic spectrum of **4** shows an absorption maximum at 380 nm ($\epsilon = 92\,000$ m^{-1} cm^{-1}) in 1,2-dichloroethane solution.

Table 2
Selected bond lengths (Å) and angles (°) for [Bu$_4$N]$_6${Cu$_6$[S$_3$C$_2$(CN)$_2$]$_6$}, **2**

Cu(1)–S(1)	2.211(2)	Cu(1)–S(1)[a]	2.239(2)
Cu(1)–S(2)	2.254(2)	Cu(1)–Cu(1)[b]	2.8770(9)
Cu(1)–Cu(1)[a]	2.8770(9)	S(1)–S(3)	2.053(2)
S(1)–Cu(1)[b]	2.239(2)	S(2)–C(1)	1.692(6)
S(3)–C(1)[b]	1.748(6)	N(1)–C(3)	1.133(9)
N(2)–C(4)	1.166(8)	C(1)–C(2)	1.408(8)
C(1)–S(3)[a]	1.747(6)	C(2)–C(4)	1.407(9)
S(1)–Cu(1)–S(1)[a]	128.55(8)	S(1)–Cu(1)–S(2)	132.45(7)
S(1)[a]–Cu(1)–S(2)	98.92(7)	S(1)–Cu(1)–Cu(1)[b]	50.15(5)
S(1)[a]–Cu(1)–Cu(1)[b]	94.60(5)	S(2)–Cu(1)–Cu(1)[b]	134.44(5)
S(1)–Cu(1)–Cu(1)[a]	109.92(5)	S(1)[a]–Cu(1)–Cu(1)[a]	49.30(5)
S(2)–Cu(1)–Cu(1)[a]	102.82(5)	Cu(1)[b]–Cu(1)–Cu(1)#1	118.605(14)
S(3)–S(1)–Cu(1)	105.56(9)	S(3)–S(1)–Cu(1)[b]	102.37(8)
Cu(1)–S(1)–Cu(1)[b]	80.55(6)	C(1)–S(2)–Cu(1)	104.8(2)
C(1)[b]–S(3)–S(1)	108.9(2)	C(2)–C(1)–S(2)	122.4(5)
C(2)–C(1)–S(3)[a]	113.2(5)	S(2)–C(1)–S(3)	124.4(4)
C(4)–C(2)–C(1)	121.0(7)	C(4)–C(2)–C(3)	117.7(6)
C(1)–C(2)–C(3)	121.3(6)	N(1)–C(3)–C(2)	179.3(10)

Symmetry transformations used to generate eqivalent atoms:
[a] $y-1$, $-x+y$, $-z+1$.
[b] $x-y+1$, $x+1$, $-z+1$.

Table 3
Selected bond lengths (Å) and angles (°) for [Bu$_4$N]$_2$[Cu(i-MNT)$_2$], **3**

Cu–S(1)	2.297(2)	Cu–S(1a)	2.297(2)
Cu–S(2a)	2.308(2)	Cu–S(2)	2.308(2)
S(1)–C(1)	1.729(8)	S(2)–C(1)	1.717(8)
N(1)–C(3)	1.145(10)	N(2)–C(4)	1.144(10)
C(1)–C(2)	1.371(10)	C(2)–C(3)	1.425(12)
C(2)–C(4)	1.434(11)		
S(1)–Cu–S(1a)	180.0	S(1)–Cu–S(2a)	102.97(9)
S(1a)–Cu–S(2a)	77.03(9)	S(1)–Cu–S(2)	77.03(9)
S(1a)–Cu–S(2)	102.97(9)	S(2a)–Cu–S(2)	180.0
C(1)–S(1)–Cu	85.2(3)	C(1)–S(2)–Cu	85.1(3)
C(2)–C(1)–S(2)	124.3(6)	C(2)–C(1)–S(1)	123.1(6)
S(2)–C(1)–S(1)	112.7(5)	C(1)–C(2)–C(3)	122.1(7)
C(1)–C(2)–C(4)	122.4(7)	C(3)–C(2)–C(4)	115.5(7)
N(1)–C(3)–C(2)	179.3(9)	N(2)–C(4)–C(2)	178.8(9)

Compound **4** also can be synthesized by mixing equal amounts of [Cu(CH$_3$CN)$_4$]PF$_6$ and [(Bu$_4$N)$_2$(i-MNT)] in an acetonitrile solution under anaerobic conditions. The yield is low, however. Most of the isolated product is **1**.

Compound **5** was isolated from a cation interchange reaction in MeOH. Single crystals suitable for X-ray diffraction were formed when one equivalent of [BzEt$_3$N]Cl was added to a solution of **4** in acetone layered with hexane.

Table 4
Selected bond lengths (Å) and angles (°) for [Bu$_4$N]$_4$[Cu$_4$(i-MNT)$_4$], **4**

Cu(1)–S(5)	2.258(4)	Cu(1)–S(4)	2.264(4)
Cu(1)–S(2)	2.316(4)	Cu(1)–Cu(2)	2.661(2)
Cu(1)–Cu(3)	2.725(2)	Cu(1)–Cu(4)	2.746(3)
Cu(2)–S(1)	2.258(4)	Cu(2)–S(7)	2.267(4)
Cu(2)–S(5)	2.303(4)	Cu(2)–Cu(3)	2.744(3)
Cu(2)–Cu(4)	2.797(3)	Cu(3)–S(3)	2.256(4)
Cu(3)–S(6)	2.271(4)	Cu(3)–S(7)	2.317(4)
Cu(3)–Cu(4)	2.657(3)	Cu(4)–S(8)	2.245(5)
Cu(4)–S(2)	2.264(5)	Cu(4)–S(3)	2.298(5)
Cu(5)–S(15)	2.253(4)	Cu(5)–S(13)	2.266(4)
Cu(5)–S(11)	2.313(4)	Cu(5)–Cu(8)	2.662(2)
Cu(5)–Cu(7)	2.730(3)	Cu(5)–Cu(6)	2.744(2)
Cu(6)–S(14)	2.258(4)	Cu(6)–S(16)	2.267(4)
Cu(6)–S(10)	2.318(4)	Cu(6)–Cu(7)	2.659(2)
Cu(6)–Cu(8)	2.749(3)	Cu(7)–S(11)	2.247(4)
Cu(7)–S(9)	2.258(5)	Cu(7)–S(16)	2.336(4)
Cu(7)–Cu(8)	2.778(3)	Cu(8)–S(10)	2.253(4)
Cu(8)–S(12)	2.256(4)	Cu(8)–S(13)	2.306(4)
S(5)–Cu(1)–S(4)	132.9(2)	S(5)–Cu(1)–S(2)	122.6(2)
S(4)–Cu(1)–S(2)	103.2(2)	S(5)–Cu(1)–Cu(2)	55.10(11)
S(4)–Cu(1)–Cu(2)	152.27(14)	S(2)–Cu(1)–Cu(2)	81.78(12)
S(5)–Cu(1)–Cu(3)	82.52(12)	S(4)–Cu(1)–Cu(3)	91.89(13)
S(2)–Cu(1)–Cu(3)	110.13(13)	Cu(2)–Cu(1)–Cu(3)	61.24(7)
S(5)–Cu(1)–Cu(4)	116.46(13)	S(4)–Cu(1)–Cu(4)	98.85(13)
S(2)–Cu(1)–Cu(4)	52.29(12)	Cu(2)–Cu(1)–Cu(4)	62.29(7)
Cu(3)–Cu(1)–Cu(4)	58.11(6)	S(1)–Cu(2)–S(7)	131.7(2)
S(1)–Cu(2)–S(5)	109.6(2)	S(7)–Cu(2)–S(5)	117.7(2)
S(1)–Cu(2)–Cu(1)	100.73(14)	S(7)–Cu(2)–Cu(1)	114.3(1)
S(5)–Cu(2)–Cu(1)	53.52(11)	S(1)–Cu(2)–Cu(3)	147.7(2)
S(7)–Cu(2)–Cu(3)	54.06(12)	S(5)–Cu(2)–Cu(3)	81.30(11)
Cu(1)–Cu(2)–Cu(3)	60.53(6)	S(1)–Cu(2)–Cu(4)	90.94(14)
S(7)–Cu(2)–Cu(4)	79.59(13)	S(5)–Cu(2)–Cu(4)	113.0(1)
Cu(1)–Cu(2)–Cu(4)	60.34(7)	Cu(3)–Cu(2)–Cu(4)	57.29(6)
S(3)–Cu(3)–S(6)	132.2(2)	S(3)–Cu(3)–S(7)	122.5(2)
S(6)–Cu(3)–S(7)	103.9(2)	S(3)–Cu(3)–Cu(4)	55.06(12)
S(6)–Cu(3)–Cu(4)	152.43(14)	S(7)–Cu(3)–Cu(4)	81.82(12)
S(3)–Cu(3)–Cu(1)	82.54(12)	S(6)–Cu(3)–Cu(1)	91.79(12)
S(7)–Cu(3)–Cu(1)	110.36(13)	Cu(4)–Cu(3)–Cu(1)	61.34(7)
S(3)–Cu(3)–Cu(2)	116.50(13)	S(6)–Cu(3)–Cu(2)	99.42(13)
S(7)–Cu(3)–Cu(2)	52.41(12)	Cu(4)–Cu(3)–Cu(2)	62.37(7)
Cu(1)–Cu(3)–Cu(2)	58.23(6)	S(8)–Cu(4)–S(2)	131.0(2)
S(8)–Cu(4)–S(3)	110.4(2)	S(2)–Cu(4)–S(3)	117.7(2)
S(8)–Cu(4)–Cu(3)	101.0(2)	S(2)–Cu(4)–Cu(3)	114.3(1)
S(3)–Cu(4)–Cu(3)	53.57(11)	S(8)–Cu(4)–Cu(1)	147.4(2)
S(2)–Cu(4)–Cu(1)	54.03(12)	S(3)–Cu(4)–Cu(1)	81.32(12)
Cu(3)–Cu(4)–Cu(1)	60.55(7)	S(8)–Cu(4)–Cu(2)	90.4(2)
S(2)–Cu(4)–Cu(2)	79.68(13)	S(3)–Cu(4)–Cu(2)	113.0(1)
Cu(3)–Cu(4)–Cu(2)	60.34(7)	Cu(1)–Cu(4)–Cu(2)	57.36(6)
S(15)–Cu(5)–S(13)	129.8(2)	S(15)–Cu(5)–S(11)	107.4(2)
S(13)–Cu(5)–S(11)	122.0(2)	S(15)–Cu(5)–Cu(8)	149.6(1)
S(13)–Cu(5)–Cu(8)	55.08(11)	S(11)–Cu(5)–Cu(8)	81.66(12)

Table 4 (continued)

S(15)–Cu(5)–Cu(7)	100.06(13)	S(13)–Cu(5)–Cu(7)	116.3(1)
S(11)–Cu(5)–Cu(7)	52.13(11)	Cu(8)–Cu(5)–Cu(7)	62.01(7)
S(15)–Cu(5)–Cu(6)	88.80(12)	S(13)–Cu(5)–Cu(6)	83.01(11)
S(11)–Cu(5)–Cu(6)	110.00(12)	Cu(8)–Cu(5)–Cu(6)	61.10(7)
Cu(7)–Cu(5)–Cu(6)	58.13(6)	S(14)–Cu(6)–S(16)	129.6(2)
S(14)–Cu(6)–S(10)	106.4(2)	S(16)–Cu(6)–S(10)	123.0(2)
S(14)–Cu(6)–Cu(7)	149.70(13)	S(16)–Cu(6)–Cu(7)	55.95(11)
S(10)–Cu(6)–Cu(7)	81.96(12)	S(14)–Cu(6)–Cu(5)	89.34(12)
S(16)–Cu(6)–Cu(5)	83.26(12)	S(10)–Cu(6)–Cu(5)	109.7(1)
Cu(7)–Cu(6)–Cu(5)	60.67(7)	S(14)–Cu(6)–Cu(8)	99.93(12)
S(16)–Cu(6)–Cu(8)	116.99(12)	S(10)–Cu(6)–Cu(8)	51.96(11)
Cu(7)–Cu(6)–Cu(8)	61.80(7)	Cu(5)–Cu(6)–Cu(8)	57.99(6)
S(11)–Cu(7)–S(9)	133.5(2)	S(11)–Cu(7)–S(16)	118.9(2)
S(9)–Cu(7)–S(16)	106.4(2)	S(11)–Cu(7)–Cu(6)	115.3(1)
S(9)–Cu(7)–Cu(6)	99.37(13)	S(16)–Cu(7)–Cu(6)	53.50(11)
S(11)–Cu(7)–Cu(5)	54.35(11)	S(9)–Cu(7)–Cu(5)	148.8(2)
S(16)–Cu(7)–Cu(5)	82.32(11)	Cu(6)–Cu(7)–Cu(5)	61.20(6)
S(11)–Cu(7)–Cu(8)	80.25(12)	S(9)–Cu(7)–Cu(8)	91.85(14)
S(16)–Cu(7)–Cu(8)	113.48(12)	Cu(6)–Cu(7)–Cu(8)	60.69(7)
Cu(5)–Cu(7)–Cu(8)	57.81(6)	S(10)–Cu(8)–S(12)	133.2(2)
S(10)–Cu(8)–S(13)	118.2(2)	S(12)–Cu(8)–S(13)	107.4(2)
S(10)–Cu(8)–Cu(5)	114.79(13)	S(12)–Cu(8)–Cu(5)	99.68(13)
S(13)–Cu(8)–Cu(5)	53.70(11)	S(10)–Cu(8)–Cu(6)	54.13(12)
S(12)–Cu(8)–Cu(6)	148.11(14)	S(13)–Cu(8)–Cu(6)	82.20(11)
Cu(5)–Cu(8)–Cu(6)	60.91(6)	S(10)–Cu(8)–Cu(7)	80.46(13)
S(12)–Cu(8)–Cu(7)	91.29(13)	S(13)–Cu(8)–Cu(7)	113.2(1)
Cu(5)–Cu(8)–Cu(7)	60.19(7)	Cu(6)–Cu(8)–Cu(7)	57.51(6)

3.2. Cluster conversion

3.2.1. UV–Vis absorption spectra

The spectra in a 1,2-dichloroethane solution at 52 °C of **4**, as shown in Fig. 1, were measured every hour, except for the last one (bottom one at 370 nm) which was obtained after 12 h. The spectra of individual species associated with the reaction sequence are shown in the inset.

The characteristics of the spectra are:

(1) The absorption maxima with extinction coefficients in parentheses for compounds **1**, **3**, **4** in 1,2-dichloroethane are listed below, measurements in other solvents showed that the spectra are not solvent dependent. **1**, 404 ($\epsilon = 86\,000$ M^{-1} cm^{-1}), 320 ($\epsilon = 60\,000$ M^{-1} cm^{-1}); **3**, 450 ($\epsilon = 15\,000$ M^{-1} cm^{-1}), 350 ($\epsilon = 80\,000$ M^{-1} cm^{-1}), 340 sh ($\epsilon = 43\,000$ M^{-1} cm^{-1}), 315 sh ($\epsilon = 25\,000$ M^{-1} cm^{-1}); **4**, 380 ($\epsilon = 92\,000$ M^{-1} cm^{-1}). The estimated $t_{1/2} = 5.5$ h for complete loss of **4** at 52 °C.

(2) The 380 nm band shows a red shift and an intensity decrease throughout the course of the experiment. Four new bands, at 450, 350, 340 and 320 nm, start to grow in after 2 h.

(3) After 13 h, the 380 nm band shifts to 404 nm (see Fig. 1), which has been

Table 5

Selected bond lengths (Å) and angles (°) for [BzEt$_3$N][Bu$_4$N]$_3$[Cu$_4$(i-MNT)$_4$], **5**

Cu(1)–S(4)	2.261(3)	Cu(1)–S(3)	2.267(3)
Cu(1)–S(2)[a]	2.305(3)	Cu(1)–Cu(2)[a]	2.717(2)
Cu(1)–Cu(2)	2.726(2)	Cu(1)–Cu(1)[a]	2.824(3)
Cu(2)–S(2)	2.269(3)	Cu(2)–S(1)	2.271(3)
Cu(2)–S(4)	2.336(3)	Cu(2)–Cu(1)[a]	2.717(2)
Cu(2)–Cu(2)[a]	2.812(3)	S(1)–C(1)	1.687(12)
S(2)–C(1)[a]	1.760(11)	S(2)–Cu(1)[a]	2.305(3)
S(3)–C(5)[a]	1.691(11)	S(4)–C(5)	1.756(11)
C(1)–C(2)	1.37(2)	C(1)–S(2)[a]	1.760(11)
C(2)–C(3)	1.40(2)	C(2)–C(4)	1.42(2)
C(3)–N(1)	1.19(2)	C(4)–N(2)	1.12(2)
C(5)–C(6)	1.38(2)	C(5)–S(3)[a]	1.691(11)
C(6)–C(8)	1.48(2)	C(8)–N(3)	1.11(2)
S(4)–Cu(1)–S(3)	128.34(13)	S(4)–Cu(1)–S(2)[a]	120.21(12)
S(3)–Cu(1)–S(2)[a]	110.70(13)	S(4)–Cu(1)–Cu(2)[a]	116.48(10)
S(3)–Cu(1)–Cu(2)[a]	100.15(10)	S(2)[a]–Cu(1)–Cu(2)[a]	52.97(9)
S(4)–Cu(1)–Cu(2)	54.92(9)	S(3)–Cu(1)–Cu(2)	147.74(10)
S(2)[a]–Cu(1)–Cu(2)	81.18(9)	Cu(2)[a]–Cu(1)–Cu(2)	62.21(6)
S(4)–Cu(1)–Cu(1)[a]	80.87(10)	S(3)–Cu(1)–Cu(1)[a]	89.31(9)
S(2)[a]–Cu(1)–Cu(1)[a]	111.06(9)	Cu(2)[a]–Cu(1)–Cu(1)[a]	58.91(5)
Cu(2)–Cu(1)–Cu(1)[a]	58.59(5)	S(2)–Cu(2)–S(1)	128.63(13)
S(2)–Cu(2)–S(4)	122.03(12)	S(1)–Cu(2)–S(4)	108.72(12)
S(2)–Cu(2)–Cu(1)[a]	54.16(9)	S(1)–Cu(2)–Cu(1)[a]	149.12(10)
S(4)–Cu(2)–Cu(1)[a]	81.94(9)	S(2)–Cu(2)–Cu(1)	115.77(10)
S(1)–Cu(2)–Cu(1)	100.38(10)	S(4)–Cu(2)–Cu(1)	52.37(9)
Cu(1)[a]–Cu(2)–Cu(1)	62.50(6)	S(2)–Cu(2)–Cu(2)[a]	79.89(9)
S(1)–Cu(2)–Cu(2)[a]	90.23(9)	S(4)–Cu(2)–Cu(2)[a]	110.53(9)
Cu(1)[a]–Cu(2)–Cu(2)[a]	59.05(5)	Cu(1)–Cu(2)–Cu(2)[a]	58.73(5)
C(1)–S(1)–Cu(2)	103.6(4)	C(1)[a]–S(2)–Cu(2)	107.3(4)
C(1)[a]–S(2)–Cu(1)[a]	112.6(4)	Cu(2)–S(2)–Cu(1)[a]	72.88(10)
C(5)[a]–S(3)–Cu(1)	104.2(4)	C(5)–S(4)–Cu(1)	104.7(4)
C(5)–S(4)–Cu(2)	112.6(4)	Cu(1)–S(4)–Cu(2)	72.71(10)
C(2)–C(1)–S(1)	120.0(9)	C(2)–C(1)–S(2)[a]	116.5(9)
S(1)–C(1)–S(2)[a]	123.5(7)	C(1)–C(2)–C(3)	121.3(13)
C(1)–C(2)–C(4)	124.3(12)	C(3)–C(2)–C(4)	114.4(13)
N(1)–C(3)–C(2)	176(2)	N(2)–C(4)–C(2)	178(2)
C(6)–C(5)–S(3)[a]	120.4(9)	C(6)–C(5)–S(4)	115.3(9)
S(3)[a]–C(5)–S(4)	124.3(7)	C(7)–C(6)–C(5)	124.6(12)

Symmetry transformations used to generate equivalent atoms:

[a] $-x+1, y, -z+1/2$

assigned as the LMCT band characteristic [27,28] of the anion of **1**, the [Cu$_8$(i-MNT)$_6$]$^{4-}$ cubane.

(4) The intensity of absorption bands at 450, 350, 340 and 320 nm increase with time. The bands at 450, 350 and 340 nm are characteristic of the red-brown material, [Cu^{II}(i-MNT)$_2$]$^{2-}$ [27,28] (see inset in Fig. 1).

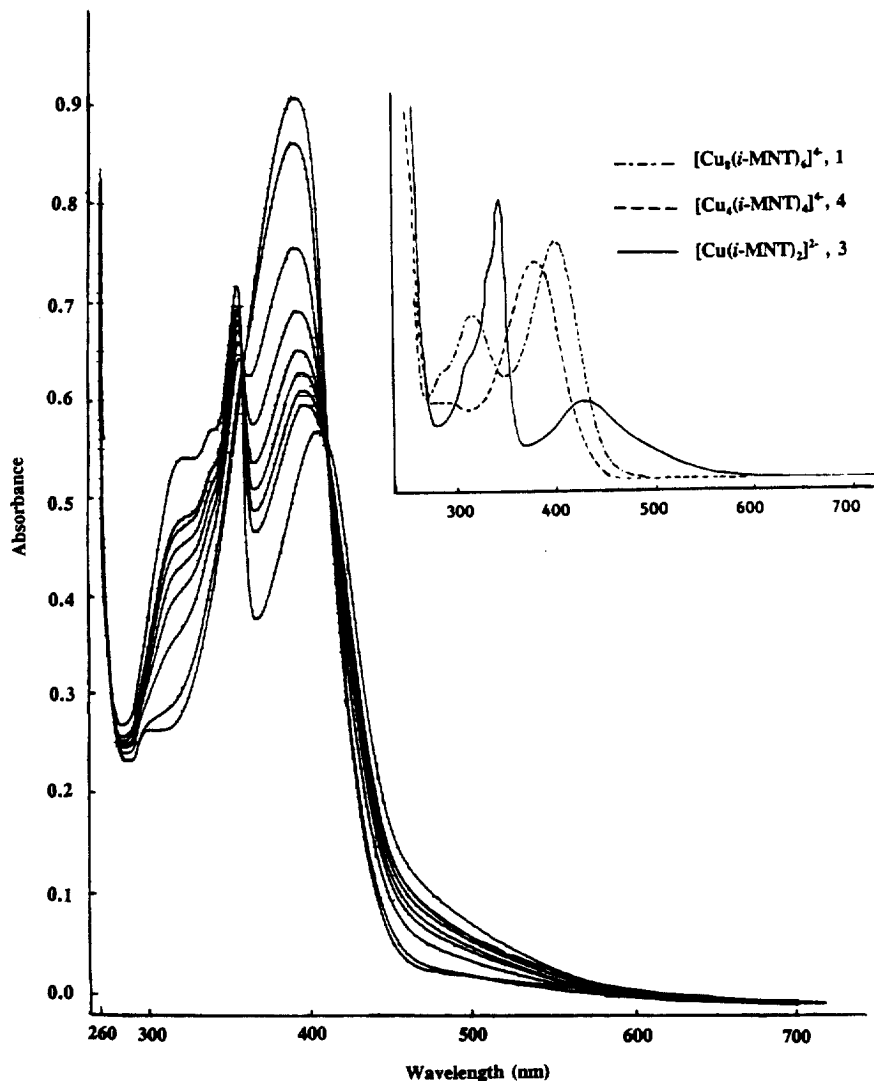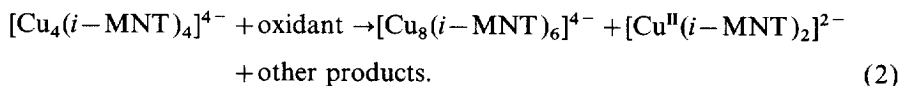(5) Isosbestic points are observed at 355 and 408 nm. The deviation in the isosbestic

Fig. 1. The UV–Vis absorption spectra of [Cu$_4$(i-MNT)$_4$], **4**, in 1,2-dichloroethane at 52 °C, recorded hourly except for the last spectrum (lowest minimum at 380 nm) which was obtained after 12 h, indicating the formation of [Cu$_8$(i-MNT)$_6$]$^{4-}$, **1**, and [Cu(i-MNT)$_2$], **3**. The spectra of the individual compounds are in the inset.

points in the last spectrum must correspond to the slow decomposition of compound **4** to compound **1** and **3**, [Cu^{II}(i-MNT)$_2$]$^{2-}$.

At room temperature (25 °C), 124 h was required to obtain a UV–Vis spectrum in dichloromethane or 1,2-dichloroethane which was identical to the 12 h spectrum recorded at 52 °C. It took even longer to obtain the spectrum of the "completed"

12 h reaction in acetone or acetonitrile. Based on this UV–Vis spectroscopic analysis, the reaction is represented by Eq. (2):

$$[\text{Cu}_4(i-\text{MNT})_4]^{4-} + \text{oxidant} \rightarrow [\text{Cu}_8(i-\text{MNT})_6]^{4-} + [\text{Cu}^{\text{II}}(i-\text{MNT})_2]^{2-}$$

$$+ \text{other products.} \tag{2}$$

In the presence of a small amount of added benzoyl peroxide, this same reaction studied at 25 °C appears complete in about 13 h (about 10 times faster). The formation of the cubane cluster $[\text{Cu}_8(i\text{-MNT})_6]^{4-}$ from the $[\text{Cu}_4(i\text{-MNT})_4]^{4-}$ cluster in solution appears to require an oxidant, either the solvent, or added oxidant (including trace amounts of oxygen in the solvent). Observation of the UV–Vis spectrum after 40 d indicated that **3** had further converted completely into **1** and the oxidized ligand.

3.2.2. Electron paramagnetic resonance spectra

Further spectroscopic evidence for the formation of $[\text{Cu}^{\text{II}}(i\text{-MNT})_2]^{2-}$, **3**, in the solutions giving $[\text{Cu}_8(i\text{-MNT})_6]^{4-}$ from **4** can be seen in the EPR spectroscopy (Fig. 2). Spectrum (b), Fig. 2 was recorded at 100 K as a sample obtained from the 1,2-dichloroethane solution after 13 h of UV–Vis experiment. Comparison of this spectrum to the authentic EPR spectrum of **3** [Fig. 2(a)] shows that some **3** is formed during the reaction of **4** as it produces **1**.

3.3. $^{13}\text{C}\{^1\text{H}\}$ nuclear magnetic resonance spectra

The cluster conversion can be followed by $^{13}\text{C}\{^1\text{H}\}$ NMR, Fig. 3. The formation of the paramagnetic **3** does not interfere with the observation of the diamagnetic Cu$^{\text{I}}$ products, although **3** itself cannot be observed by NMR. The spectra were
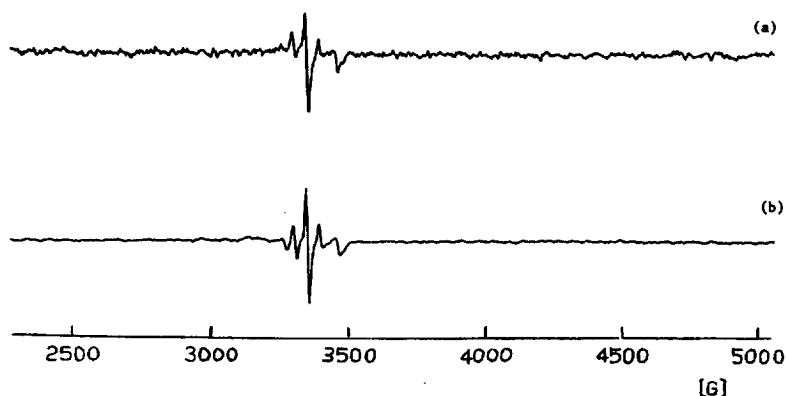

Fig. 2. The EPR spectra at 100 K. (a) Top, authentic sample of **3** in MeOH; (b) bottom, solution of **4** from the UV–Vis experiment after 13 h.
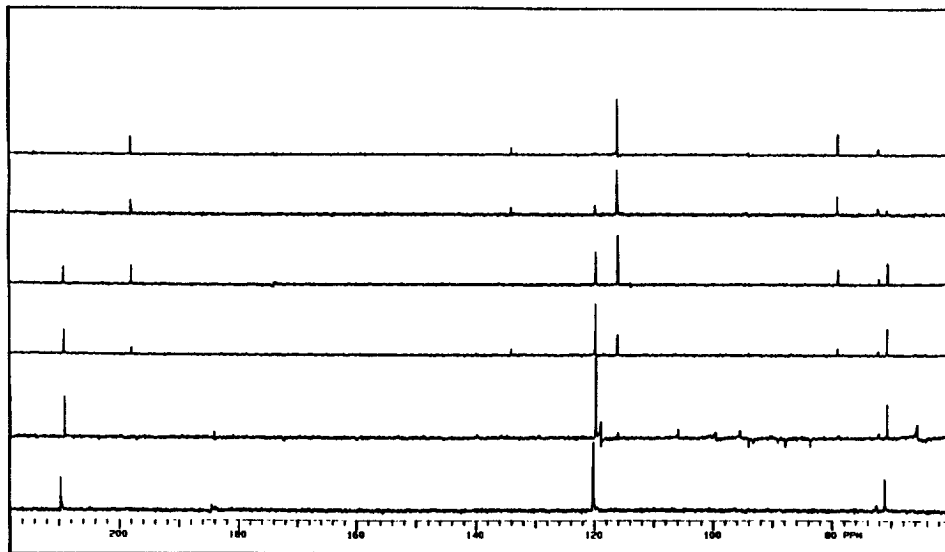
Fig. 3. The $^{13}C\{^1H\}-NMR$ spectra in CD_2Cl_2 solution indicating the formation of Cu_8 from Cu_4. The spectra were recorded after 1, 3, 13, 22, 29 and 35 days (from bottom to top).

recorded in CD_2Cl_2 solution after 1, 3, 13, 22, 29 and 35 days (from bottom to top). The resonances at 209.5, 120 and 70.8 ppm belong to the carbon atoms of the $[Cu_4(i\text{-MNT})_4]^{4-}$ species. A small peak at 116 ppm, which is the resonance of the cyanocarbon atoms in $[Cu_8(i\text{-MNT})_6]^{4-}$, appears after three days. After 13 days, two new peaks at 79(=C) and 199(CS_2) ppm are detected and the intensity of the 116 ppm peak increases. Obviously both **4** and **1** are present in the solution. The intensity of peaks which belong to **4** start to decrease as time increases. Only peaks (199, 116 and 79 ppm) belonging to the carbon atoms of **1** are observed in the solution after 35 days. The resonances at 72.5 and 134 ppm are attributed to solvent impurities. The estimated $t_{1/2}$ for the loss of **4** from these NMR measuremnts is 500 h.

3.3.1. Peak broadening

The $^{13}C\{^1H\}$-NMR spectra show some peak broadening in the presence of **3**. The spectrum of the i-MNT ligand is presented in Fig. 4(a), in MeOH (0.10 M). The peaks at 140 and 67 ppm are impurities. Upon adding $[Bu_4N]_2[Cu^{II}(i\text{-MNT})_2]$, **3**, (17.5 mg, 10^{-2} M), peak broadening occurs, Fig. 4(b). **3** itself is not completely soluble and its spectrum is not observed. Addition of 1 ml of CH_2Cl_2 to the MeOH solution to insure dissolution of **3** gives spectrum Fig. 4(c) in which the i-MNT ligand signals appear absent or strongly shifted. The $[^nBu_4N]^+$ cation and the peaks of the solvents MeOH and CH_2Cl_2 are sharp as seen in Fig. 4(d). Ligand exchange with the paramagnetic Cu^{II} site is very likely the cause for the disappearance of the
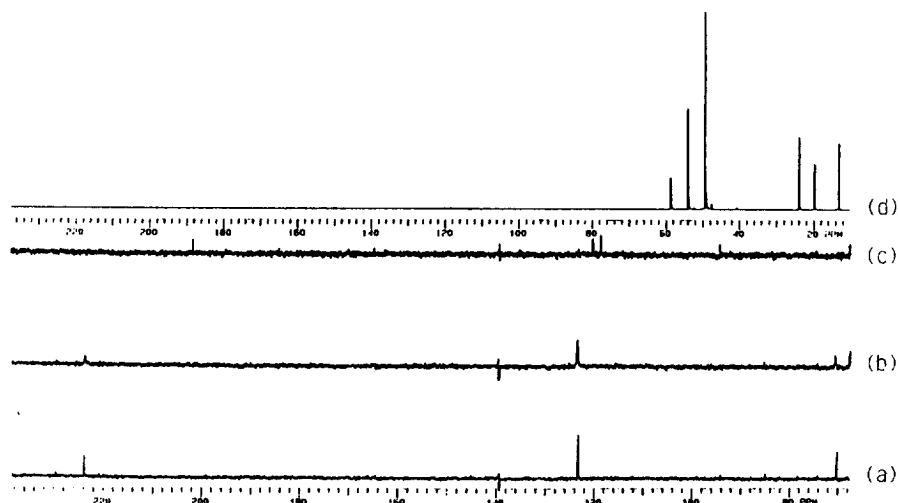
Fig. 4. The $^{13}C\{^{1}H\} - NMR$ spectra in the presence of 3: (a) [$^{n}Bu_4N$]$_2$[i-MNT] in MeOH; (b) after adding 3 ; (c) after adding CH_2Cl_2; and (d) the spectra of the quaternary ammonium salt and the solvent molecules.

resonances of the ligand signals in Fig. 4(b) while the line broadening in Fig. 4(c) probably is a result of sample inhomogeniety.

4. Structural results

4.1. Crystal structure of [Bu$_4$N]$_6$[Cu$_6$(S,i-MNT)$_6$]

A thermal ellipsoid drawing of the novel sulfur-rich hexanuclear cluster is presented in Fig. 5. The molecule contains six trigonally coordinated copper atoms linked together into a 12-membered ring by the six sulfur atoms of the bridging sulfur-rich i-MNT ligands. There is a crystallographically imposed bar 3 symmetry at the center of the molecule which has S_6 molecular symmetry. The bridging sulfur atoms can be subdivided into two sets, one pointed up and one directed down. This repetitive pattern, in combination with a bend at the copper and bridging sulfur atoms, produces the observed cyclic structure. The six copper atoms lie within $\pm 0.172(1)$ Å of a common plane, three up and three down.

As shown in Fig. 6, there are three idealized octahedral cages formed by the S atoms in 2. The central octahedron which is made from the six bridging sulfur atoms, S(1), S(1a), S(1b)...S(1e), is surrounded by another octahedron produced by the six catenated sulfur atoms, S(3), S(3a), S(3b)...S(3e), adjacent to the carbon atom of the CS_2 moiety. The third octahedron of S atoms, atoms coordinated to Cu^I, S(2), S(2a), S(2b)...S(2e), is twisted relative to the other two. A slight distortion from a regular octahedron is found in the central S_6 cage in which the differences
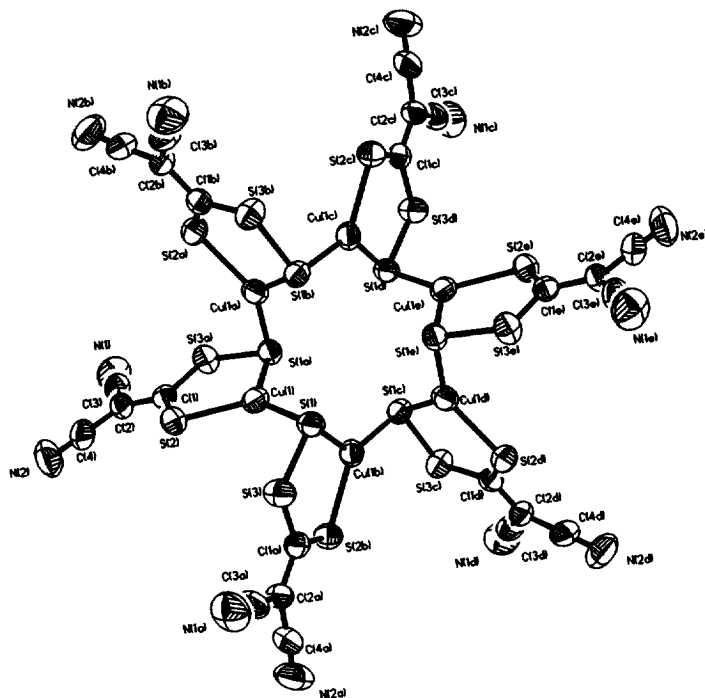
Fig. 5. Thermal ellipsoid drawing of $[Cu_6(S,i\text{-MNT})_6]^{6-}$, **2** (50% probability).

of the S–S edge separations are only 0.160 Å (3.849–4.009 Å). Two triangular faces of the octahedron are equilateral, those perpendicular to the C_3 axis, the other six faces are isosceles. The copper atoms sit on the six long edges. The mean distance between the two equilateral triangles of the central sulfur octahedron is 3.337 Å.

The three coordinate Cu^I atoms are located at a distance of only 0.035(8) Å from the plane of the sulfur atoms, S(1)-S(2)-S(1a), to which they are coordinated. Pronounced deviations from trigonal symmetry are most evident in the Cu–S bond lengths and S–Cu–S angles. Two of the Cu–S bond lengths Cu(1)–S(2) and Cu(1)–S(1a) are nearly equal [2.254(2); 2.239(2)] while the third Cu(1)–S(1) bond length is 2.211(2) Å. The S–Cu–S angle between the two longer bonds [98.92(7)°] is appreciably smaller than the other two angles of 132.45(7)° and 128.55(8)°. The shortest Cu–Cu distance in **2** is 2.877(9) Å which is very similar to the shortest Cu–Cu distance [15] in the homocubane cluster, **1**. The S–S catenated sulfur distance, 2.053(2) Å, is within the normal range found for sulfur-rich dithiolate metal complexes (Table 6). The CuSSCS chelate rings are tilted relative to each other by 57.9°. Only one-sixth of the anion and one cation are in the asymmetric unit, other atoms are related to these by the bar 3 symmetry.

As is evident from the space-filling model shown in Fig. 7, complex **2** has a small central hole, with an approximate diameter of 2–3 Å. In the final difference Fourier map, some residual electron density, $+0.267e\ A^{-3}$ is located in the vicinity of Cu(1).
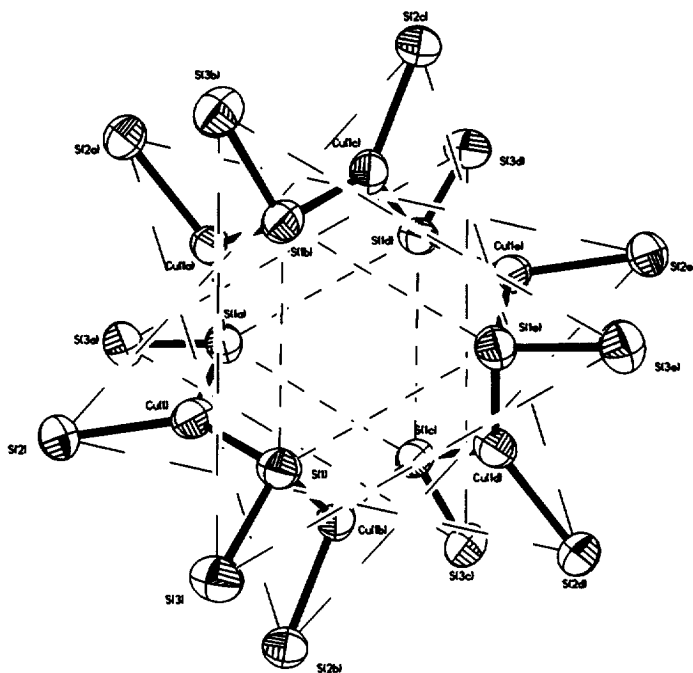
Fig. 6. Sketch of the idealized octahedral sulfur cages in $[Cu_6(S, i\text{-}MNT)_6]^{6-}$, **2**.

The small interior of **2**, together with the negligible electron density located around the copper center, indicates that no guest molecule or atom is present [51] in the crystal studied, although guest ions have been found in cubane $[Cu_8(dtp)_6X]^{n-}$ clusters [16,17]. A unit cell packing diagram reveals that the molecules stack along the c-axis with their interior holes overlapping each other, so that an infinite channel is generated in the crystal lattice. A stereoview down the c-axis highlights this feature (supplementary material only). The $[Cu_6(S,i\text{-}MNT)_6]^{6-}$ anion is surrounded symmetrically by the six Bu_4N^+ counterions.

4.2. Crystal structure of $[Bu_4N]_2[Cu(i\text{-}MNT)_2]$

The structure of the anion in **3** is shown in Fig. 8. The compound **3** crystallizes in the monoclinic space group $P2_1/n$ with two molecules per unit cell. The anion in **3** is planar with the copper ion located on the center of symmetry. Two four-membered CuSCS rings formed by the chelated i-MNT ligands and the copper atom are related to each other by sharing the common vertex of the copper atom. The sum of the angles within the ring is $360°$ as required by symmetry, and the S–Cu–S angle is acute, $77.03(9)°$. The Cu–S distances are identical [$2.308(2)$ and $2.297(2)$ Å] within the limits of error. A distorted square planar coordination environment around the copper ion is evident in the S–Cu–S angles, $77.03(9)°$ and $102.97(9)°$,

Table 6
A list of sulfur-rich dithiolate metal complexes which have been structurally characterized

Compounds S–S	Distance (å)	a
I. Perthiocarboxylate		
1. Fe(S$_2$C-p-tolyl)$_2$(S$_3$C-p-tolyl) [98]	2.09	Chelating
3. Ni(S$_3$CPh)$_2$ [52,99]	2.022(3)	Chelating
Zn(S3CPh)$_2$ [52,99]	2.007(3)	
3. Ni(S$_2$C-p-^{i}Pr-C$_6$H$_4$)(S$_3$C-p-^{i}Pr-C$_6$H$_4$) [33]	2.016(4)	Chelating
Zn(S$_3$C-p-^{i}Pr-C$_6$H$_4$)$_2$ [33]	2.008(4)	
4. [CuS$_3$C-o-tolyl]$_4$ [34]	2.050(1)	$\mu_2;\mu_1$
5. [AgS$_3$C-o-tolyl]$_4$ [35]	2.041(5)	$\mu_2;\mu_1$
[Ag$_{1.76}$Cu$_{2.24}$(S$_3$C-o-tolyl)$_4$] [35]		
6. MoO(S$_2$CPh)(S$_3$CPh) [100]	2.048(1)	Chelating
7. [Cu(S$_3$C-2,4,6-(Me)$_3$C$_6$H$_2$)]$_4$ [36]		$\mu_2;\mu_1$
8. [Cu(S$_3$C-C$_{10}$H$_7$)]$_4$ [37]		$\mu_2;\mu_1$
9. [Cu$_2$(S$_3$C-o-tolyl)(S$_2$C-o-tolyl)bipy] [38]	2.037(4)	$\mu_2;\mu_1$
[(CuS$_3$C-o-tolyl)$_2$Phen] [38]	2.053(2)	
[(CuS$_3$C-o-tolyl)Phen] [38]	2.012(2)	
II. Perthiocarbamate		
1. Os$_2$(S$_2$CNEt$_2$)$_3$(S$_3$CNEt$_2$)(μ-S$_5$) [39]	2.16	$\mu_2;\mu_1$
[Os$_2$(S$_3$CNMe$_2$)$_2$(S$_2$CNMe$_2$)$_3$]PF$_6$ [39]	2.166,2.141	
2. [Os$_2$(S$_2$CNEt$_2$)$_3$(S$_3$CNEt$_2$)$_2$]BPh$_4$ [40]	2.05(2),2.13(1)	$\mu_2;\mu_1$
3. [Re$_2$(μ-S$_3$CNR$_2$)$_2$(S$_2$CNR$_2$)$_3$][O$_3$SCF$_3$] [41]		$\mu_2;\mu_1$
(R = Me,i-Bu)	2.264(7),2.194(7)	
III.Perthiophosphate		
1. [HB(Me$_2$Pz)$_3$]MoO(S$_3$P(OEt$_2$)$_2$) [42]	2.396(3)	Chelating
IV. Perthio-ethylene dithiolate		
1. [Cu$_5$(S,^{t}BuDED)$_4$]$^{1-}$ [20]	2.055	$\mu_2;\mu_2$
[AuCu$_4$(S,^{t}BuDED)$_4$]$^{1-}$ [20]	2.094	
[Cu$_4$(S,^{t}BuDED)$_3$]$^{2-}$ [20]	2.076(4)	
2. [Cu$_6$(S,i-MNT)$_6$]$^{6-}$(this work)	2.055(3)	$\mu_2;\mu_1$
3. MoCp$_2$S$_3$C$_2$(2-quinoxaline)(COMe) [43,44]	2.074(2)	Chelating
V. Perthiocarbonate		
1. [Ni(CS$_4$)$_2$]$^{2-}$ [45]	2.064(2)	Chelating
2. [PhCH$_2$NEt$_3$][(Mn(CO)$_3$(CS$_4$))$_2$] [46]	2.070(4)	$\mu_2;\mu_1$
3. [Et$_4$N][Mn(CS$_4$)$_2$Cl] [47]	2.048(2)	Chelating
4. [PPh$_4$]$_2$[trans-(S)Mo(η^2-CS$_4$)$_2$] [48,49]	2.101(5)	Chelating
[PPh$_4$]$_2$[syn-cis-Mo$_2$(S)$_2$(μ-S)$_2$(η^2-CS$_4$)$_2$] [48,49]	2.005(2)	
[PPh$_4$][Et$_4$N][cis-(S)-Mo(η^2-CS$_4$)$_2$] [48,49]	2.105(4)	
[Et$_4$N]$_2$[Mo$_2$O$_2$(μ-S)$_2$(η^2-CS$_4$)(η^2-CS$_3$)] [48,49]	2.061(9)	
VI. Perthiooxalate		
Ph$_4$P[(ptoMe)Ni(i-dtoMeacac)] [50]	2.013(8)	Chelating

^{a} Ligand bridging mode.

Abbreviations used in this table and the text: i-MNT: [S$_2$CC(CN)$_2$]$^{2-}$, 1,1-dicyanoethylene-2,2-dithioate; ^{t}Bu-DED: [S$_2$CC(COO^{t}Bu)$_2$]$^{2-}$, 1,1-di-t-butoxyl-ethylene-2,2-dithioate; i-dtoMe: [S$_2$CC(O)OMe]$^{1-}$, o-Methyl-1,1-dithiooxalate; DTS: [SOC$_2$OS]$^{2-}$, 1,2-dioxoethylene-1,2-dithioate.
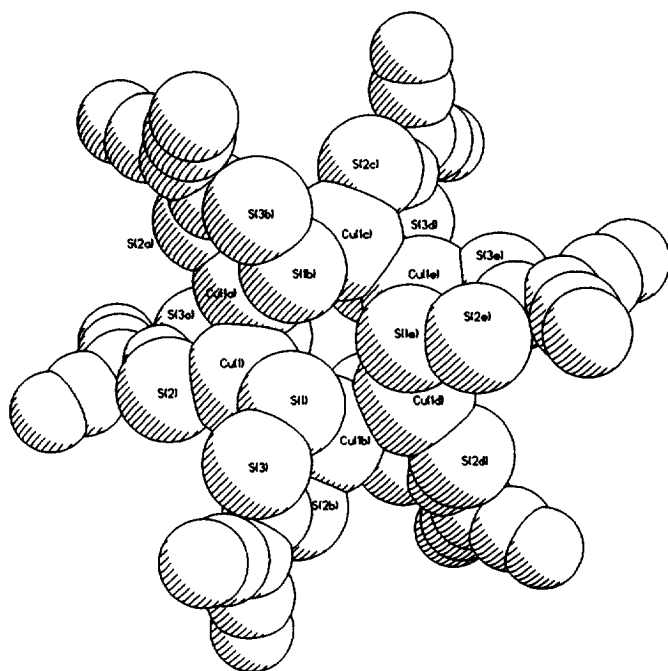
Fig. 7. Sketch of a space-filling model for $[Cu_6(S,i\text{-MNT})_6]^{6-}$, **2**, using standard atom radii.

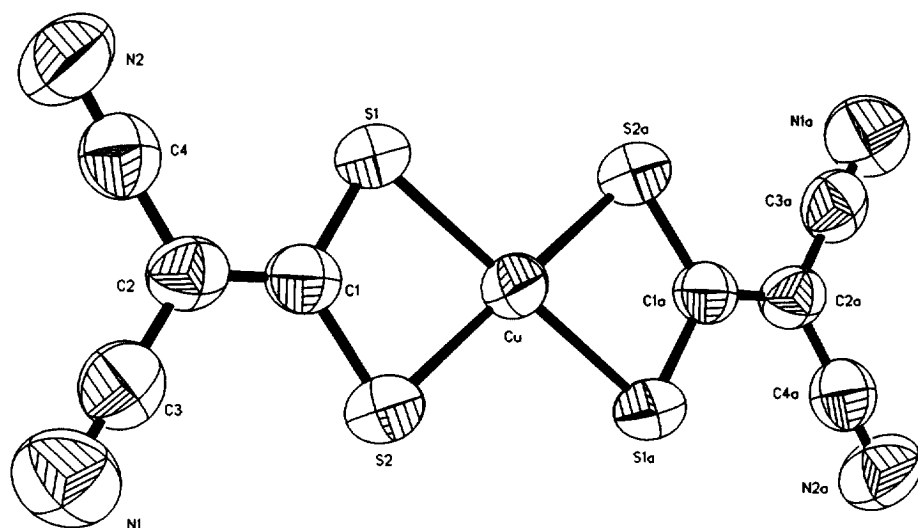
Fig. 8. Thermal ellipsoid drawing of $[Cu(i\text{-MNT})_2]^{2-}$, **3** (50% probability).

respectively. A typical carbon–carbon double bond (1.371 Å) is found in the chelated *i*-MNT ligands.

4.3. Crystal structures of [Bu₄N]₄[Cu₄(i-MNT)₄], 4 and [BzEt₃N][Bu₄N]₃[Cu₄(i-MNT)₄]

The structure of the anion of **5** is shown in Fig. 9. Both compounds **4** and **5** crystallize in the $C2/c$ space group. There are two crystallographically independent Cu_4 units in the asymmetric unit for compound **4**. Only half of the Cu_4 unit is present for **5**, the other half is generated by the crystallographically imposed two-fold symmetry. Both anions have idealized S_4 point group symmetry. Basically the structures of both of the anions are the same. The anion reveals discrete units of four copper atoms, at the vertices of a distorted tetrahedron, with four *i*-MNT groups acting as "tridentate" ligands. A sulfur atom of each ligand coordinates to only one copper atom while the other S atom bridges across the Cu_3 triangle to two adjacent copper atoms, so that each copper atom is in an approximately trigonal geometry with an almost planar arrangement of the three sulfur atoms coordinated to it. The displacements of the metal atoms from the plane through the sulfur atoms range from 0.101(6) to 0.114(2) Å. The Cu–Cu distances associated with the copper atoms bridged by the sulfur atoms bonded to C range from 2.718 to 2.725 Å; the remaining Cu–Cu distances bridged by the disulfide S atoms range from 2.814 to 2.825 Å. The intraligand S–S "bite" distance averages 3.029 Å.
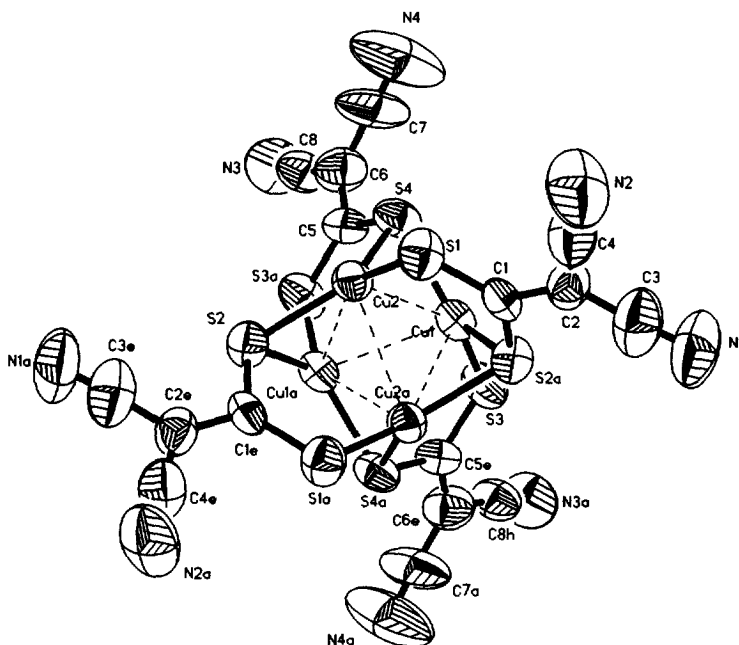
Fig. 9. Thermal ellipsoid drawing of $[Cu_4(i\text{-MNT})_4]^{4-}$, **4** (50% probability).

5. Discussion

5.1. Syntheses

The elegant Cu^I 1,1-dithiolate cluster studies by Coucouvanis et al. [19] utilizing the ligand "'Bu—DED" demonstrated that with non-interacting Bu_4N^+ cations the $[Cu_8(S,L)_6]^{4-}$ clusters could be obtained but unfortunately could not be structurally characterized. In the presence of alkali metal ions, the sulfur-rich tetranuclear clusters, $[Cu_4(S,{}^tBu\text{-}DED)_3]^{2-}$, could be isolated and structurally characterized [20]. If the sulfur insertion reaction into the Cu_8S_{12} cluster were general, it seemed possible that $[Cu_8(S,i\text{-}MNT)_6]^{4-}$ clusters might be isolated. However, neither $[Cu_8(S,L)_6]^{4-}$ nor $[Cu_4(S,L)_3]^{2-}$ could be obtained. One of the reasons for this may be the synthetic approach itself with the different 1,1-dithiolate ligands. Base is required in the synthesis of $[Cu_6(S,i\text{-}MNT)_6]^{6-}$. No base is needed in the synthesis of $[Cu_8(S, {}^tBu\text{-}DED)_6]^{4-}$. The different basicities of the sulfur-rich ligands may play an important role in the different clusters formed. This is especially true if the S insertion is a result of nucleophilic attack on the S_2C carbon as was demonstrated to be the case with Ni^{II} and Zn^{II} dithiocarboxylates [52].

Hydrolysis reactions have been used extensively in the synthesis of many sulfur-rich 1,1-dithiotoluate metal complexes [33,34,38]. A remarkable phase-transfer-catalyzed reaction of $[Mn_2(CO)_9Br]^-$ with sulfur afforded a sulfur-rich $\{[Mn(CO)_3(CS_4)]_2\}^{2-}$ complex [46], although the mechanism for this intriguing reaction remains unclear. Presumably compound **2** is obtained by a hydrolysis reaction in which the hydroxide ion removes a proton from acetonitrile to generate $[CH_2CN]^-$. The polysulfide anion, $(base)S_x^-$, is presumably obtained by nucleophilic attack of $[CH_2CN]^-$, or base generally, upon the S_8 ring of sulfur [53]. It is well established that the reaction of anionic polysulfide with many transition metal 1,1-dithiolate complexes produces sulfur-rich species with a chelate ring expansion [54]. The path for formation of **2** from **1** presumably involves a similar nucleophilic attack at the S_2C carbon atom of $[Cu_8(i\text{-}MNT)_6]^{4-}$. Beyond this, speculation into the formation of $[Cu_6(S,i\text{-}MNT)_6]^{6-}$ is unwarranted.

Coucouvanis [20] showed that the oxidation of the $[(Cu_4L_3)^{2-}]_n$ ($n = 1$ or 2; $L = S, {}^tBu—DED$) clusters with either Cu^{II} or Au^{III} results in the formation of the mixed-metal, mixed-valence coinage metal clusters $[Cu_5L_4]^-$ and $[AuCu_4L_5]^-$ that contain the sulfur-rich ligands. The structures of both anions are similar and consist of Cu_5 and $AuCu_4$ rectangular pyramids with four bridging sulfur-rich ligands spanning and nearly bisecting the triangular faces. In both structures the formally trivalent ion at the apex of the pyramid, (Cu^{III} or Au^{III}) is four coordinate and square planar. A similar mixed-valence cluster product was not detected in the oxidation of $[Cu_6(S,i\text{-}MNT)_6]^{6-}$ with Cu^{II}. The only products identified were CuS and $[Cu_8(i\text{-}MNT)_6]^{4-}$.

The instability of the Cu^{II}–S bond makes isolation of Cu^{II}–thiolate complexes fairly difficult. This bond easily undergoes homolysis, with reduction of the Cu^{II} ion to Cu^I and the formation of disulfide, Eq. (3):

$$2Cu^{II}—SR \rightarrow 2Cu^I + RSSR. \tag{3}$$

Therefore, by using sterically bulky thiolate ligands which form disulfides only with difficulty, one may stabilize Cu^{II}–SR compounds. However, it has been found that 1,1 or 1,2-dithiolate ligands also have a tendency to stabilize high-valency copper complexes. Among the compounds that have been structurally characterized include $[Cu^{III}(MNT)_2]^-$ [55], $[Cu^{III}(DED)_2]^-$ [56], $[Cu^{III}(DTO)_2]^-$ [57], $[Cu^{II}(DTO)_2]^{2-}$ [57], $Cu^{II}(dtc)_2$ [58]. The electronic properties of **3** which were studied by Gray et al. [27] is a example of a well characterized, relatively stable Cu^{II}–thiolate complex, although it does produce $[Bu_4N]_4[Cu_8(i\text{-MNT})_6]$, **1**, in solution as described in the original synthesis of the $[^nPr_4N]^+$ salt[2] [59,60] of **1**.

In addition to $SPPh_3$, the desulfurization product of $[Cu_6(S,i\text{-MNT})_6]^{6-}$ using PPh_3 produces the $[Cu_4(i\text{-MNT})_4]^{4-}$ cluster. Kanodia and Coucouvanis [61] reported that removal of the extra sulfur atoms from the sulfur-rich ligands in the $[Cu_4(S, {}^tBu\text{-DED})_3]^{2-}$ cluster produces the homocubane, $[Cu_8({}^tBu\text{-DED})_6]^{4-}$. If a $[Cu_4({}^tBu\text{-DED})_4]^{4-}$ species is an intermediate in this system, it was not isolated. Attempts to isolate an octahedral $[Cu_6(i\text{-MNT})_6]^{6-}$ cluster with a geometry presumably like that of the well known $[Ag_6(i\text{-MNT})_6]^{6-}$ cluster [62,63], have not succeeded to date.

Efforts to synthesize the sulfur rich product of the $[Cu_4(i\text{-MNT})_4]^{4-}$ have led to hexanuclear $[Cu_6(S,i\text{-MNT})_6]^{6-}$. It appears that the sulfur oxidation product (with base) of either **4** or **1** is **2**. It is possible that $[Cu_4(i\text{-MNT})_4]^{4-}$ initially is converted to Cu_8 in solution, then $[Cu_6(S,i\text{-MNT})_6]^{6-}$ is isolated from by reaction of the cubane with sulfur in the presence of base. Although the $[Cu_4(S,{}^tBu\text{-DED})_4]^{4-}$ has been isolated and used as a "cluster-ligand" to synthesize mixed-valence clusters by Coucouvanis et al. [20], no structure has been reported.

It has long been known that octanuclear cage molecules with a cubane-type metal skeleton are obtained by reaction of Cu^I with dinegative 1,1 or 1,2-dithiolate ligands. Characterized compounds include: $[Cu_8(i\text{-MNT})_6]^{4-}$ [15], $[Cu_8(DED)_6]^{4-}$ [64,65], $[Cu_8(DTS)_6]^{4-}$ [64,65], and $[Cu_8(MNT)_6]^{4-}$ [66]. In contrast to this, tetranuclear clusters with a tetrahedral metal core generally have been isolated from reactions of Cu^I with uninegative 1,1-dithioacid ligands although octanuclear cages with centered anions have been described recently [16,17]. Tetranuclear examples include $Cu_4(dtc)_4$ [23], $Cu_4(dtp)_4$ [67], and $Cu_4(S_2CC_7H_7)_4$ [68]. Compound **4** is the first tetranuclear Cu^I cluster structurally characterized with four dianionic 1,1-dithiolate ligands.
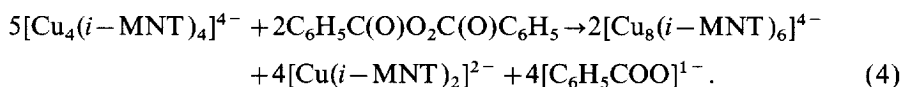
5.2. Cluster conversion

Since both $[Cu_8(i\text{-MNT})_6]^{4-}$ and $[Cu(i\text{-MNT})_2]^{2-}$ are produced during the recrystallization of $[Bu_4N]_4[Cu_4(i\text{-MNT})_4]$ from 1,2-dichloroethane, further study of this reaction was conducted. The UV–Vis studies indicate that the tetranuclear i-MNT cluster very slowly converts into the octanuclear homocubane and **3**, a result confirmed by EPR measurements. The two isosbestic points observed (Fig. 1) strongly suggest that there are no other spectroscopically observable species present in solu-

---

[2] These early papers along with Ref. [27] observed this product to be formed from Cu^{II}, but assumed it was tetranuclear (see Ref. [9]).

tion except compounds **1**, **3** and **4** during the initial conversion process. ^{13}C–NMR results substantiate the formation of **1** from **4** in solution but the reaction takes much longer at the higher concentrations required for this study. This reaction also is different from the reversible transformation of $[Cu_8(S,^tBu-DED)_6]^{4-}$ to $[Cu_4(S,^tBu\text{-}DED)_3]^{2-}$ reported by Coucouvanis et al. [19] which apparently is controlled by the Lewis acid–Lewis base behavior of the cations present in solution.
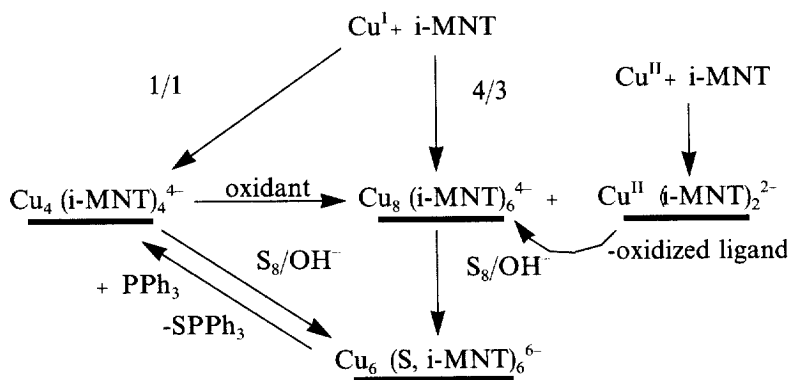
The difficulties associated with studying a very dilute solution maintained anaerobic over period of several days suggested to us that oxidation might be involved in the cluster conversion even before we identified the presence of **3**. Therefore benzoyl peroxide was added. It was found to enhance the conversion rate, decreasing the time for complete conversion to the cubane by an estimated factor of 10. (Benzoyl peroxide was not added in the NMR studies.) A stoichiometric reaction representing he Cu_4 conversion with benzoyl peroxide is given by Eq. (4). Our study did not determine product ratios.

$$5[Cu_4(i-MNT)_4]^{4-} + 2C_6H_5C(O)O_2C(O)C_6H_5 \rightarrow 2[Cu_8(i-MNT)_6]^{4-}$$
$$+ 4[Cu(i-MNT)_2]^{2-} + 4[C_6H_5COO]^{1-}. \qquad (4)$$

The difference between the observed conversion rate at room temperature observed in the UV–Vis ($t_{1/2} \sim 60$ h) and the NMR ($t_{1/2} \sim 500$ h) experiments presumably is associated with different concentrations used in the measurements which are $\sim 10^3$ greater in the NMR studies. The much longer half-life of **4** at the higher NMR concentrations (reaction completion required about 40 days) suggests that a spontaneous loss of ligands, a reaction which is expected to be first order in tetranuclear cluster concentration, is not involved in the rate controlling step to produce the cubane. However, a process which is of higher order in the concentration of **4** cannot be ruled out from this study. The presence of the oxidant benzoyl peroxide greatly increases the conversion rate (approximately 10 times faster at room temperature and about as fast as the 55 °C result). However, a quantitative measurement of the benzoyl peroxide concentration was not performed. The qualitative slowing of the reaction in acetonitrile and acetone, even at the low concentrations associated with the UV–Vis spectral measurements, further implicates a rate enhancement by oxidation since these solvents are themselves not oxidants and probably also reduce the activity of dioxygen compared with methylene dichloride. In the NMR measurements over several days, the CD_2Cl_2 may function as the oxidant (although trace amounts of dioxygen also could be present). Failure to observe the free ligand, which would result from the simple conversion of **4** to **1**, is expected from the EPR results and the UV–Vis spectral measurements which identified **3** as a product in the solution, and the NMR results of the ligand which shows signal loss in the presence of **3**. While we do know that the conversion is promoted by an oxidant, and that **3** formed at least initially, the complex sequence of reactions associated with the conversion process remains to be fully understood.

UV–Vis measurements of **4** at ambient temperature over more than 40 days further indicate that $[Bu_4N]_2[Cu(i\text{-}MNT)_2]$, **3**, will decompose into the cubane, **1**,

and the oxidized ligand. This result confirms the original synthetic study [59]. The ^{13}C-NMR experiments further corroborate the UV–Vis results of the transformation of Cu^{II} into the cubane, **1**, although the oxidized ligand could not be identified in the NMR spectrum (see NMR results) due to exchange with the paramagnetic **3**. Clearly the cubane is the thermodynamic product of the reaction of either Cu^{I} or Cu^{II} with i-MNT ligands. Based on our results a sequence of reactions leading to the formation of the cubane and related products is summarized below.

$$Cu^{I} + i\text{-MNT}$$

$$1/1 \qquad\qquad 4/3 \qquad Cu^{II} + i\text{-MNT}$$

$$Cu_4 (i\text{-MNT})_4{}^{4-} \xrightarrow{\text{oxidant}} Cu_8 (i\text{-MNT})_6{}^{4-} + \quad Cu^{II} (i\text{-MNT})_2{}^{2-}$$

$$+\ PPh_3 \qquad S_8/OH^- \qquad\qquad S_8/OH^- \qquad \text{-oxidized ligand}$$

$$-SPPh_3$$

$$Cu_6 (S, i\text{-MNT})_6{}^{6-}$$

5.3. Structures

The cyclic structure of **2** is uncommon in copper–sulfur cluster chemistry. Many hexanuclear Cu^I clusters containing sulfur donor ligands have been characterized structurally. They are listed in Table 7. Most of the clusters have near-octahedral skeletons of the metal cores except for the last two listed which have a geometry that can be roughly described as edge-sharing bi-tetrahedra. The near trigonal-planar CuS_3 geometry around each copper is commonly found. Most of the ligands chelate across a triangular metal face bonding to three copper atoms. The mean distances between two parallel trinuclear copper planes are 2 A. or longer in each structure previously reported. Instead of the common bridging mode observed for most of the complexes listed in Table 7, the ligands in **2** use only the terminal sulfur atom of the disulfide moiety to bridge to two copper atoms. This type of bridge also is observed with sulfur-rich 1,1-dithio acid ligands [34–37,39–41].
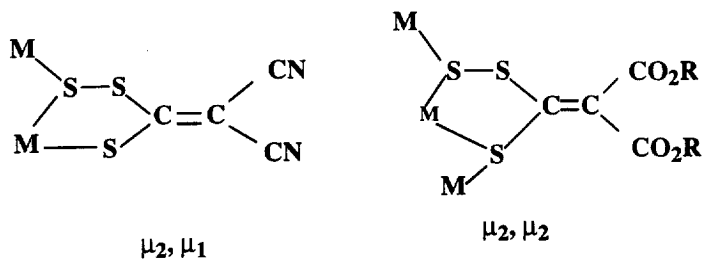
μ_2, μ_1 μ_2, μ_2

Table 7

Structures of hexanuclear Cu^I complexes containing sulfur donor ligands

Compounds	Distance (Å) between plane	Structure[a] of Cu_6 core	Geometry[b] of each copper (donor set)[c]
$[Cu_6(R_2NCOS)]_6$ R:Et,Pr [69]	2.199	o	Trigonal($2S_b$,O_t)
$[Cu_6(C_5H_4NS)_6]$ [70]	2.513(4)	o-t.a.	Trigonal ($2S_b$, N_t)
$[Cu_6(C_5H_5N_2OS)_6]$ [71]	2.957(7)	o-t.a.	Trigonal ($2S_b$, N_t)
$[Cu_6(C_6H_7N_2S)_6]$ [72]		o-t.a	Trigonal ($2S_b$, N_t)
$[Cu_6(C_9H_6NS)_6]$ [73]		o-t.a.	Trigonal ($2S_b$, N_t)
$[Cu_6(C_5H_3NSSiMe_3)_6]$ [74]		s.t.t.	Trigonal ($2S_b$, N_t)
$\{Cu_6[BuSC(S)NPh]_6\}$ [75]	2.302(3)	o-t.a.	Trigonal ($S2_b$, N_t)
$\{CuPhNC(S)N[(C_2H_4)_2O]\}_6$ [76]	1.964(3)	o-t.a.	Trigonal ($2S_b$, N_t)
$[PPh_4][Cu_6In_3(SEt)_{16}]$ [77]	2.529(1)	o-t.a.	Trigonal ($3S_b$) Tetrahedral ($4S_b$)
$\{Cu[\mu_2SC(=NPh)(OC_6H_4Me)]\}_6$ [78]	2.547(3)	o-t.a.	Trigonal ($2S_b$, N_t)
$[VS_4(CuPPh_3)_5(CuCl)Cl_2]$ [79]	3.415(9)	o-t.a.	Trigonal ($2S_b$, Cl_t) Tetrahedral ($2S_b$, Cl_b, P_t)
$[(MoS_4)Cu_6I_8][PPh_4]_4$ [80]	2.832(9)	o-t.a.	Trigonal ($2S_b$, I_t) Tetrahedral ($2S_b$, I_b, I_t)
$[NMe_4]_5[MoS_4(CuCl)_6Cl_3]$ [81]	2.712(8)	o-t.a.	Trigonal ($2S_b$, Cl_t) Tetrahedral ($2S_b$, $2Cl_t$)
$[Bu_4N]_6[Cu_6(S,i\text{-}MNT)]_6$	0.345(2) this work	planar	Trigonal ($2S_b$, S_t)
$[Et_4N]_2[Cu_6Mo_6O_6S_{19}]\cdot C_3H_7NO$ [82]	2.582(6)	g.t.t.	Tetrahedral($4S_b$)
$\{W_2Cu_6S_6(SCMe_3)_2\}(O)_2(Ph_3P)_4$ [83]	2.902(3)	o-t.a.	Trigonal ($3S_b$) Tetrahedral ($3S_b$, P_t)
$[Cu_6(S_4)_3S_5][PPh_4]_2$ [84,85]		e.s.b.t.	
$\{Cu_3[SC_6H_4(CH_2NMe_2)]_2(C\equiv Bu^t)\}_2$ [86,87]		e.s.b.t.	

[a] O = Octahedral, t.a. = trigonal antiprismatic, e.s.b.t. = edge-sharing bitetrahedral, s.t.t. = staggered two trigonal, g.t.t. = gauched two trigonal.
[b] By assuming no Cu–Cu bonding.
[c] Suffixes b and t denote bridging and terminal coordination modes, respectively.

The ligand bridging mode in **2** is different from that observed with the S,^{t}Bu-DED ligands. The latter is represented as S,S;S′,S′(μ_2–S; μ_2–S) as found in the mixed-valence coinage metal clusters[13] of $Cu_5L_4^-$ and $AuCu_4L_4^-$ (L = S,^{t}Bu-DED), and in the $Cu_4L_3^{2-}$ cluster. (Each ligand S atom in these clusters is bridging and spanning a triangular metal atom face.) The sulfur-rich i-MNT ligand appears unable to support such a product. As far as the structure of the ligand bridging mode is concerned, the S,i-MNT ligand appears to be more closely related to the sulfur-rich 1,1-dithio (uninegative charge) ligands.

Since the six bridging sulfur atoms in both compound **2** and the $Cu_6(SOCNR_2)_6$ (R = Et, Pr)[69] clusters are located on the vertices of an idealized octahedron, the geometry of the six copper atoms in these two clusters is differentiated by their positions on the different edges of an octahedron. In the $Cu_6(SOCNR_2)_6$ cluster, the copper atoms sit on the six edges of two parallel triangular sulfur planes. The six copper atoms in **2** are located on the six "belt" edges of the S atom octahedron, the octahedral "belt" of the six triangular faces which do not contain the three-fold

axis, nearly in the plane which goes through the middle of these edges. If the sulfur atom cage in **2** were a perfect octahedron the six copper atoms would lie on the plane. The 0.345(2) Å distance observed between the two copper triangular planes on the three-fold axis illustrates the small distortion of the sulfur cage from an octahedron.

[$Cu_6(SOCNR_2)_6$]   [$Cu_6(S, i\text{-MNT})_6$]$^{6-}$
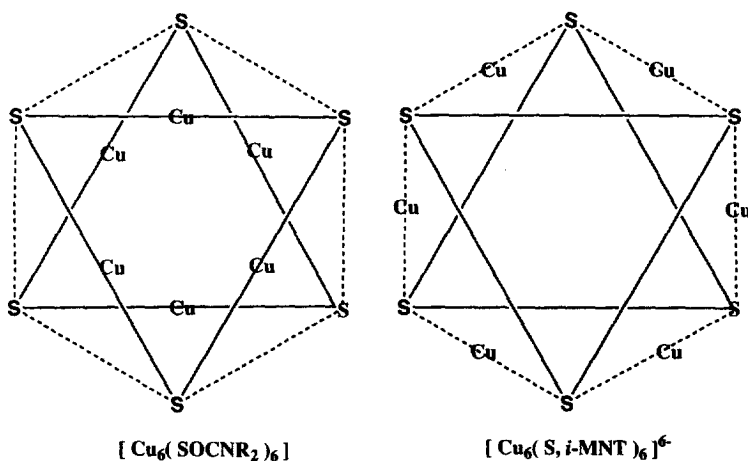
The most unusual structural feature in **2** is this nearly regular hexagonal geometry of the Cu_6 metal array. With other metal ions, however, a hexagonal arrangement of metal ions in sulfur complexes is common. Some prominent examples of clusters having a regular hexagon of six metal atoms bridged by pairs of μ_2 thiolate ligands, such that each metal atom has a planar coordination, include $Ni_6(SR)_{12}$ (R = Et [88], Pr [89], $Pd_6(SPr^i)_{12}$ [90,91], $M_6(SCH_2CH_2OH)_{12}$ (M = Ni or Pd) [92], and $Ni_6(SCH_2CH(Me)OH)_{12}$ [93].

Few cyclic structures of Cu^I with sulfur-containing ligands have been reported [94]. Most of these clusters contain "Cu–S" core units of stoichiometry Cu_2S_2 [95], Cu_3S_3 [96] and Cu_4S_4 [97]. Compound **2** is the only cyclic molecule observed to date with the core unit stoichiometry of Cu_6S_6.

Winge et al. [7,8] have described the arrangement for copper within mammalian MT in terms of two domains. Stillman et al. [9–11] has provided supporting evidences from circular dichroism (CD) and emission data that mammalian MT binds first six Cu^I atoms, then 12, to form stable complexes. The structure of **2** provides a new Cu_6 model to be considered for the copper binding site of mammalian MT.
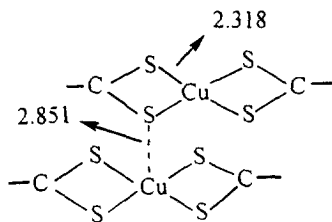
There is a significant difference between the solid state structures of $[Cu^{II}(i\text{-}MNT)_2]^{2-}$, **3**, and $Cu^{II}(dtc)_2$. In $Cu(dtc)_2$, [58], each centrosymmetrically related pair of copper atoms share sulfur atoms. Each copper atom has a distorted tetragonal–pyramidal coordination by four sulfur atoms, at distances ranging between 2.297 and 2.339 Å, and a fifth apical sulfur atom at 2.851 Å. In **3**, there is no intermolecular Cu–S interaction in the solid state, with the shortest distance being 8.097 Å. This feature might be a result of the unit cell packing caused by the bulky quaternary ammonium cations which occupy much of the space and prevent any intermolecular Cu–S interaction.

6. Conclusion

The novel sulfur-rich cluster, $[Cu_6(S,i\text{-}MNT)_6]^{6-}$, has been produced by reaction of $[Cu_8(i\text{-}MNT)_6]^{4-}$, **1**, and sulfur under basic conditions. This hexanuclear Cu^I cluster has a unique cyclic structure previously unknown in Cu–S chemistry and provides a new Cu_6 model to be considered for Cu^I binding in proteins. Both the clusters $[Cu_8(i\text{-}MNT)_6]^{4-}$ and $[Cu_8(^tBu\text{-}DED)_6]^{4-}$ have a similar structural feature — a distorted cube of copper atoms embedded within a cluster of 12 sulfur atoms which lie on the vertices of a distorted icosahedron. However, their oxidation products with sulfur, $[Cu_6(S,i\text{-}MNT)_6]^{6-}$, **2**, and $[Cu_8(S,^tBu\text{-}DED)_6]^{4-}$, respectively, are different. Removal of one of the catenated sulfur atoms from compound **2** produces a new, anionic tetranuclear cluster, $[Cu_4(i\text{-}MNT)_4]^{4-}$, **4**. This molecule further converts into the homocubane cluster, **1**, and a Cu^{II} species, $[Cu(i\text{-}MNT)_2]^{2-}$ **3**, after a few days in solution. The structural and spectroscopic evidence reported here indicates that the homocubane cluster, **1**, is the "thermodynamic sink" for the reaction of either Cu^I or Cu^{II} with i-MNT ligands and that **4** converts into **1** by a process accelerated by oxidation.

7. Supplementary material available

Tables of crystallographic data, atomic coordinates, anisotropic displacement parameters, bond distances and angles for **2–5** (200 pages) and a stereo view down the c-axis of **2**.

References

[1] J.M. Walshe, in: J. Peisach, P. Aisen, W.E. Plumberg, (Eds.), The Biochemistry of Copper, Academic Press, New York, 1966, p. 475.

[2] J.H. Menke, G.K. Steigleder, D.R. Weakley, J.H. Sung, Pediatrics 29 (1962) 764.

[3] M.C. Linder, Biochemistry of Copper, Plenum Press, New York, 1991.

[4] W. Hoffmann, Rubber Technology Handbook, Hanser, Münich, 1989.

[5] T. Colclough, IEC. Res. 26 (1987) 1888.

[6] K.T. Tamai, E.B. Gralla, L.M. Ellerby, J.S. Valentine, D.J. Thiele, Proc. Natl Acad. Sci. USA 90 (1993) 8013.

[7] K.B. Neilson, D.R. Winge, J. Biol. Chem. 260 (1985) 9698.

[8] K.B. Neilson, C.L. Atkin, D.R. Winge, J. Biol. Chem. 260 (1985) 5432.

[9] M.J. Stillman, A.Y.C. Law, W. Cai, A.J. Zelazowski, Experientia Suppl. 52 (1987) 203.

[10] Z. Gasyna, A. Zelazowski, A.R. Green, F. Ough, M.J. Stillman, Inorg. Chim. Acta. 153 (1983) 115.

[11] A.R. Green, A. Presta, Z.M. Gasyna, Inorg. Chem. 33 (1994) 4159.

[12] G.N. George, J. Byrd, D.R. Winge, J. Biol. Chem. 263 (1988) 8199.

[13] J.R. Casas-Hinet, S. Hu, D. Hamer, R.L. Karpel, Biochemistry 31 (1992) 6617.

[14] K.H. Nakagawa, C. Inouye, B. Hedman, M. Karim, T.D. Tullius, K.D. Hodgeson, J. Am. Chem. Soc. 113 (1991) 3621.

[15] L.E. McCandlish, E.C. Bissel, D. Coucouvanis, J.P. Fackler Jr., K. Knox, J. Am. Chem. Soc. 90 (1968) 7357.

[16] C.W. Liu, T. Stubbs, R.J. Staples, J.P. Frackler Jr., J. Am. Chem. Soc. 117 (1995) 9778–9779.

[17] I. Haiduc, D.B. Sowerby, S.-F. Lu, Polyhedron 14 (1995) 3389.

[18] F.A. Cotton, G. Wilkinson, Advanced Inorganic Chemistry, 5th Edn, Wiley, New York, 1988, pp. 608–609.

[19] S. Kanodia, D. Coucouvanis, Inorg. Chem. 11 (1982) 469.

[20] D. Coucouvanis, S. Kanodia, D. Swenson, S.-J. Chan, T. Studemann, N.C. Baenziger, R. Pedelty, M. Chu, J. Am. Chem. Soc. 24 (1993) 11271.

[21] D. Coucouvanis, D. Swenson, N.C. Baenziger, R. Pedelty, M.L. Cattery, S. Kanodia, Inorg. Chem. 28 (1989) 2829.

[22] D. Coucouvanis, D. Swenson, N.C. Baenziger, R. Pedelty, M.L. Cattery, J. Am. Chem. Soc. 99 (1977) 8097.

[23] R. Hesse, Ark. Kemi. 20 (1963) 481.

[24] J.P. Fackler, Jr., A.Elduque, R. Dávila, David (C.W.) Liu, C. Lopez, T. Grant, C. McNeal, R. Staples, T. Carlson, in: A.J. Welch, S.K. Chapman (Eds.), The Chemistry of the Copper and Zinc Triads, The Royal Society of Chemistry, 1993, p.186.

[25] D.F. Shriver, M.A. Drezdzon, The Manipulation of Air-Sensitive Compounds, 2nd ed., Wiley, New York, 1986.

[26] G.J. Kubas, Inorg. Syn. 19 (1979) 90.

[27] B.G. Werden, E. Billig, H.B. Gray, Inorg. Chem. 5 (1966) 78.

[28] A. Avdeef, J.P. Fackler Jr., Inorg. Chem. 17 (1978) 2182.

[29] G.M. Sheldrick, SHELX93, Program for the Refinement of Crystal Structures, University of Göttingen, Göttingen, Germany, 1993.

[30] G.M. Sheldrick, Acta Crystallogr. A46 (1990) 467.

[31] J.M. Burke, J.P. Fackler Jr., Inorg. Chem. 11 (1972) 3000.

[32] J.P. Fackler Jr., J.A. Fetchin, J.A. Smith, J. Am. Chem. Soc. 92 (1970) 2910.

[33] A.M. Manotti Lanfredi, A. Tiripicchio, N. Marsich, A. Camus, Inorg. Chim. Acta. 142 (1988) 269.

[34] N. Marsich, G. Pellizer, A. Camus, A.M. Manotti Lanfredi, F. Ugozzoli, Inorg. Chim. Acta 169 (1990) 171.

[35] J.A. Schuerman, F.R. Fronczek, J. Selbin, J. Inorg. Chim. Acta 148 (1988) 177.

[36] K. Tang, H. Gan, X. Xu, G. Zhou, Y.Q. Tang, Sci. Sin., Ser. B. (Engl. Ed.) 27 (1984) 456.

[37] X.L. Jin, Y.Y. Jin, Y.Q. Tang, Acta. Chim. Sin. 44 (1986) 580.

[38] A. Camus, N. Marsich, A.M. Manotti Lanfred, F. Ugozzoli, Inorg. Chim. Acta 175 (1990) 193.

[39] L.J. Maheu, L.H. Pignolet, J. Am. Chem. Soc. 102 (1980) 6346.

[40] L.J. Maheu, L.H. Pignolet, Inorg. Chem. 18 (1979) 3626.

[41] L. Wei, T.R. Halbert, H.H. Murry III, E.I. Stiefel, J. Am. Chem. Soc. 112 (1990) 6431.

[42] A.A. Eagle, L.J. Laughlin, C.G. Young, E.R.T. Tiekink, J. Am. Chem. Soc. 114 (1992) 9195.

[43] P.S. Pilato, K.A. Eriksen, M.A. Greaney, E.I. Stiefel, S. Goswami, L. Kilpatrick, T.G. Spiro, E.C. Taylor, A.L. Rheingold, J. Am. Chem. Soc. 113 (1991) 9372.

[44] T.R. Halbert, W.-H. Pan, E.I. Stiefel, J. Am. Chem. Soc. 105 (1983) 5476.

[45] D. Coucouvanis, P.R. Patil, M.G. Kanatzidis, B. Betering, N.C. Baenziger, Inorg. Chem. 24 (1985) 24.

[46] H. Alper, F. Sibtain, F.W.B. Einstein, A.C. Willis, Organometallics 4 (1985) 604.

[47] S.-B. Yu, R.H. Holm, Polyhedron 12 (1993) 263.

[48] D. Coucouvanis, M.E. Draganjac, J. Am. Chem. Soc. 104 (1982) 6820.

[49] D. Coucouvanis, M.E. Draganjac, S.M. Koo, A. Toupadakis, A.I. Hadjikyriacou, Inorg. Chem. 31 (1992) 1186.

[50] J. Piotraschke, P. Strauch, G. Zahn, E. Hoyer, Z. Anorg. Allg. Chem. 620 (1994) 505.

[51] M.F. Hawthorne, Z. Zheng, Acc. Chem. Res. 30 (1997) 267.

[52] J.P. Fackler Jr., J.A. Fetchin, D.C. Fries, J. Am. Chem. Soc. 94 (1972) 7323.

[53] R.E. Davis, in: G. Nickless (Ed.), Inorganic Sulfur Chemistry, Elsevier, New York, 1968, p. 85.

[54] D. Coucouvanis, Prog. Inorg. Chem. 16 (1979) 302.

[55] J.D. Forrester, A. Zalkin, D.H. Templeton, Inorg. Chem. 3 (1964) 1507.

[56] D. Coucouvanis, F.J. Hollander, M.C. Caffery, Inorg. Chem. 15 (1976) 1853.

[57] M.G. Kanatzidis, N.C. Baenziger, D. Coucouvanis, Inorg. Chem. 24 (1985) 2680.

[58] M. Bonamico, G. Dessy, A. Mugnoli, A. Vaciago, L. Zambonelli, Acta. Crystallogr. 19 (1985) 886.

[59] G.W. Watt, B.J. McCormick, J. Inorg. Nucl. Chem. 27 (1965) 898.

[60] J.P. Fackler Jr., D. Coucouvanis, J. Am. Chem. Soc. 88 (1966) 3913.

[61] S. Kanodia, Ph.D. Dissertation, University of Iowa, Iowa City, 1978.

[62] H. Dietrich, W. Storck, G. Manecke, J. Chem. Soc., Chem. Comm. (1982) 1036.

[63] H. Zhang, X. Yu, Jiegou Hauxue 6 (1987) 98.

[64] F.J. Hollander, D. Coucouvanis, J. Am. Chem. Soc. 99 (1977) 6268.

[65] F.J. Hollander, D. Coucouvanis, J. Am. Chem. Soc. 96 (1974) 5646.

[66] H. Dietrich, W. Storck, G. Manecke, Makroml. Chem. 182 (1981) 2371.

[67] S.L. Lawton, W.J. Rohrbaugh, G.T. Kokotailo, Inorg. Chem. 11 (1972) 612.

[68] A. Camus, N. Marsich, Inorg. Chim. Acta 161 (1989) 87.

[69] R. Hesse, U. Aava, Acta Chem. Scand. 24 (1970) 1355.

[70] S. Kitagawa, M. Munakata, H. Shimono, S. Matsuyama, H.J. Masuda, Chem. Soc., Dalton Trans. (1990) 2105.

[71] S. Kitagawa, Y. Nozaka, M. Munakata, S. Kawata, Inorg. Chim. Acta 197 (1992) 169.

[72] R. Castro, M.L. Duran, J.A. Garcia-Vazquez, J. Romero, A. Sousa, E.E. Castellano, J. Chem. Soc., Dalton Trans. (1992) 2559.

[73] S. Kitagawa, S. Kawata, Y. Nozaka, M.J. Munakata, J. Chem. Soc., Dalton Trans. (1993) 1699.

[74] E. Block, M. Gernon, H. Kang, J. Zubieta, Angew. Chem. Int. Ed. Engl. 27 (1988) 1342.

[75] J. Willemse, W.P. Bosman, J.H. Noordik, J.A. Cras, Rec. Trav. Chim. Pays-Bas. 102 (1983) 477.

[76] J. Willemse, W.P. Bosman, J.H. Noordik, J.A. Cras, Rec. Trav. Chim. Pays-Bas. 100 (1981) 240.

[77] W. Hirpo, S. Ohingra, M.G. Kanatzidis, J. Chem. Soc., Chem. Comm. (1992) 557.

[78] N. Narasimhamurthy, A.G. Samuelson, H.J. Manohar, J. Chem. Soc., Chem. Comm. (1989) 1803.

[79] C.D. Scattergood, P.G. Bonney, J.M. Slater, C.D. Garner, W. Clegg, J. Chem. Soc., Chem. Comm. (1987) 1749.

[80] A. Müller, E. Krickemeyer, A. Hildebrand, H. Bogge, K. Schneider, M.J. Lemke, J. Chem. Soc., Chem. Comm. (1991) 1685.

[81] S. Bernes, F. Secheresse, Y. Jeannin, Inorg. Chim. Acta 191 (1991) 11.

[82] X. Wu, B. Wang, B. Zheng, J. Lu, J. Struct. Chem. 7 (1988) 47.

[83] S. Du, N. Zhu, P. Chen, X. Wu, Angew. Chem. Int. Ed. Engl. 31 (1992) 1085.

[84] G. Henkel, P. Betz, B. Krebs, J. Chem. Soc., Chem. Comm. (1984) 314.

[85] A. Müller, M. Römer, H. Bögge, E. Krickemeyer, D. Bergmann, J. Chem. Soc., Chem. Comm. (1984) 348.

[86] D.M. Knotter, A.L. Spek, D.M. Grove, G. van Koten, J. Chem. Soc., Chem. Comm. (1989) 1738.

[87] D.M. Knotter, A.L. Spek, D.M. Grove, G. van Koten, Organometallics 11 (1992) 4083.

[88] P. Woodward, L.F. Dahl, E.W. Abel, B.C. Cross, B.C. Am. Chem. Soc. 87 (1965) 5251.

[89] H. Feld, A. Leute, D. Rdding, A. Benninghoven, G. Henkel, T. Krüger, B. Krebs, Z. Naturforsch 47b (1992) 929.

[90] R.G. Hayter, F.S. Humiec, J. Inorg. Nucl. Chem. 26 (1964) 807.

[91] N. Kunchur, Acta Crystallogr. B24 (1968) 1623.

[92] R.O. Gould, M.H. Harding, J. Chem. Soc. (A) (1970) 875.

[93] R.M. Taylor, Ph.D. Dissertation, University of Edinburgh, UK, 1967.

[94] I. Dance, K. Fisher, Prog. Inorg. Chem. 41 (1994) 637.

[95] I.G. Dance, P.J. Guerney, A.D. Rae, M.L. Scudder, Inorg. Chem. 22 (1983) 2883.

[96] I.G. Dance, L.J. Fitzpatrick, M.L. Scudder, J. Chem. Soc., Chem. Comm. (1983) 546.

[97] I.G. Dance, Polyhedron 5 (1986) 1037.

[98] M. Bonamico, G. Dessy V. Fares, L. Scaramuzza, J. Chem. Soc. A. (1971) 3191

[99] D.C. Fries, J.P. Fackler, Jr., Chem. Comm. (1971) 276.

[100] M. Tatsumisago, G. Matsubayashi, T. Tanaka, S. Nishigaki, K. Nakatsu, J. Chem. Soc., Dalton Trans. (1982) 121.